Dalton Transactions

Accepted Manuscript

This article can be cited before page numbers have been issued, to do this please use: N. Leygue, A. Boulay, C. Galaup, E. Benoist, S. Laurent, L. Vander Elst, B. Mestre-Voegtlé and C. Picard, *Dalton Trans.*, 2016, DOI: 10.1039/C6DT00405A.

ROYAL SOCIETY OF CHEMISTRY

www.rsc.org/dalton

View Article Online
DOI: 10.1039/C6DT00405A

Optical and relaxometric properties of monometallic (Eu^{III}, Tb^{III}, Gd^{III}) and heterobimetallic (Re^{I}/Gd^{III}) systems based on a functionalized bipyridine-containing acyclic ligand

Nadine Leygue, Alexandre Boulay, Chantal Galaup, Eric Benoist, Sophie Laurent, Luce Vander Elst, Béatrice Mestre-Voegtlé and Claude Picard

The photophysical and relaxometric properties in aqueous solutions of Ln-BPMNTA complexes and a derived Re^{I}/Gd^{III} dinuclear complex are reported.

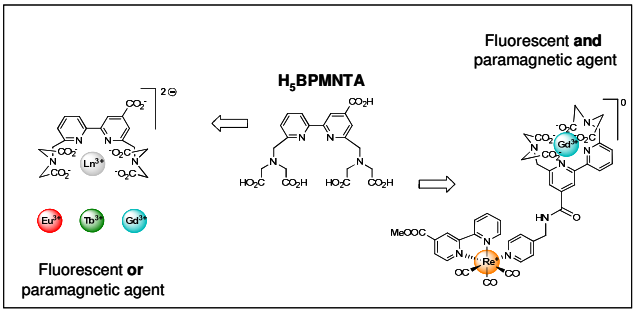

Optical and relaxometric properties of monometallic (Eu^{III}, Tb^{III}, Gd^{III}) and heterobimetallic (Re^{I}/Gd^{III}) systems based on a functionalized bipyridine-containing acyclic ligand†

Nadine Leygue,[a,b] Alexandre Boulay,[a,b] Chantal Galaup,[a,b] Eric Benoist,[a,b] Sophie Laurent,[c,d] Luce Vander Elst,*[c,d] Béatrice Mestre-Voegtlé,* ‡[a,b] and Claude Picard*[a,b]

[a]CNRS; Laboratoire de Synthèse et Physico-Chimie de Molécules d'Intérêt Biologique, SPCMIB, UMR-5068; 118 Route de Narbonne, F-31062 Toulouse cedex 9, France.
E-mail: picard@chimie.ups-tlse.fr (CP), beatrice.mestre@lcc-toulouse.fr (BMV)
[b]Université de Toulouse; UPS, Laboratoire de Synthèse et Physico-Chimie de Molécules d'Intérêt Biologique, SPCMIB; 118 route de Narbonne, F-31062 Toulouse cedex 9, France.
[c]NMR and Molecular Imaging Laboratory, Department of General, Organic and Biomedical Chemistry, University of Mons, 23 Place du Parc, B-7000 Mons, Belgium.
E-mail: luce.vanderelst@umons.ac.be
[d]Center for Microscopy and Molecular Imaging (CMMI), Rue Adrienne Bolland, 8, B-6041 Gosselies, Belgium

†Electronic supplementary information (ESI) available: Spectroscopic characterization of ligands, Re and Gd complexes and dinuclear Re/Gd complex, influence of concentration and temperature on the relaxation rate of Gd complexes, parameters obtained from the theoretical fitting of the O-17 and ^{1}H NMR data of dinuclear Re/Gd complex. See DOI:

‡Present Address: CNRS, Laboratoire de Chimie de coordination (LCC), UPR CNRS 8241, 205 route de Narbonne, 31077 Toulouse cedex 4, France.

View Article Online
DOI: 10.1039/C6DT00405A

Abstract

A series of lanthanide complexes of $[LnL(H_2O)]^{2-}$ composition with Ln = Eu^{III}, Tb^{III} or Gd^{III} has been studied for determining their photophysical and relaxometric properties in aqueous solution. The bifunctional ligand L (H_5BPMNTA) is an acyclic chelator based on a central functionalized 2,2'-bipyridine core and two iminodiacetate coordinating arms. The mono-aqua Eu^{III} and Tb^{III} complexes display attractive spectroscopic properties with excitation wavelength at 316 nm, similar excited state lifetimes and overall quantum yields (in the range 0.5-0.6 ms and 10-13%, respectively) in Tris buffer (pH 7.4). The proton longitudinal relaxivity, r_1, of the Gd^{III} complex is 4.4 mM^{-1} s^{-1} at 20 MHz and 310 K which is comparable to that of the clinically used Gd-DTPA (Magnevist®). Interestingly, the water exchange rate between the coordination site and the bulk solvent is very fast ($K_{ex} = 2.6 \times 10^8$ s^{-1} at 310 K). The ability of the complex to bind noncovalently to human serum albumin (HSA) was also examined by relaxometric measurements. We also report the synthesis and properties of a bimetallic complex based on Gd-BPMNTA and $Re^{I}(bpy)(CO)_3$ components. In this system, the Re core exhibits interesting photophysical properties (λ_{em} = 588 nm, Φ = 1.4%) and the Gd-BPMNTA core displays improved relaxivity (r_1 = 6.6 mM^{-1} s^{-1} at 20 MHz and 310 K), due to an increase of the rotational correlation time. Besides these appealing optical and relaxometric properties, the presence of a reactive function on the structure nominates this potential dual imaging probe for conjugation to biomolecules or nanomaterials.

View Article Online
DOI: 10.1039/C6DT00405A

Introduction

Over the last three decades, the use of metallic ions has been fundamental in the development of the major imaging techniques such as MRI (magnetic resonance imaging), Optical imaging (fluorescence microscopy) or SPECT (single photon emission computed tomography) and PET (positron emission tomography) nuclear imaging. As far as M^{III} ions are concerned, this is due to the unique magnetic properties of Gd^{III} ions (high magnetic moment coupled with a long electronic relaxation time), luminescent properties of Ln^{III} ions such as Eu^{III}, Tb^{III}, Nd^{III} or Yb^{III} (long-lived excited states and emission in the visible or near-infrared regions) and radiochemical properties of ^{111}In (γ emitter), ^{86}Y or ^{68}Ga (β^+ emitters).[1-4]

Interestingly, the above mentioned M^{III} ions can be chelated by a unique ligand, mainly a poly(amino)poly(carboxylate) scaffold, leading the way to multimodal imaging based on the use of metal complexes cocktails. In these systems, a simple exchange of the metal in the complex allows multimodal imaging analyses to be undertaken, taking advantage of the specific strengths of each imaging modality and overcoming their limitations (sensitivity, spatial and temporal resolutions, depth penetration).[5] Examples of ligands include the linear diethylenetriaminepentaacetic acid (H_5DTPA) and macrocyclic 1,4,7,10-tetraazacyclododecane-1,4,7,10-tetraacetic acid (H_4DOTA). In particular, the Gd^{III}-DTPA complex (marketed as Magnevist®) was introduced in 1988 as the first intravenous MRI contrast agent authorized for clinical use, and is in widespread use around the world.[6] DTPA derivatives where a chromophoric unit is introduced through an acetate arm were employed with other lanthanide metals (principally Eu^{III} and Tb^{III}) for an access to luminescent probes.[7] In nuclear medicine, the ^{111}In-DTPA-octreotide conjugate (commercially available under the name Octreoscan^{TM}) has been approved by FDA as a SPECT agent for imaging neuroendocrine tumours.[8] Radiocomplexes derived from ^{86}Y or ^{68}Ga and DTPA were also used for PET imaging applications.[9] H_4OCTAPA (Figure 1) is another noticeable example of acyclic poly(amino)poly(carboxylate) ligand which was assessed as a M^{III} chelator in various metal complexes like radiopharmaceuticals (^{111}In, ^{177}Lu), luminescent probes (Eu^{III}, Tb^{III}) and MRI contrast agent (Gd^{III}).[4,10]

In the course of our research on the design of M^{III} ions chelating systems with potential biomedical imaging applications, we were interested in the development of acyclic chelators derived from the DTPA backbone where a functionalized pyridine or 2,2'-bipyridine unit is substituted for the central dimethylene aminoacetate core (H_5PMNTA, H_5BPMNTA, Figure 1).[11,12] The H_5BPMNTA chelator is composed of (i) an octadentate N_4O_4 donor set adequate

View Article Online
DOI: 10.1039/C6DT00405A

for efficient complexation of lanthanides and related ions such as In^{III} or Y^{III} ions and (ii) an aromatic carboxylic acid function, in position 4 of the bis-heterocycle, available to covalently attach the ligand or the complex to a targeting moiety such as peptides, antibodies or nanoparticles. We have recently synthesized an ^{111}In-BPMNTA core conjugated to the C-terminal function of a cholecystokinin tetrapeptide (CCK4) which targets tumours overexpressing the cholecystokinin receptor subtype 2 (CCK2R).[13] In this work, we have successfully demonstrated that this bioconjugate may be used *in vivo* as a molecular nuclear imaging agent for the visualization of CCK2R positive tumours on small animal. Moreover, biodistribution and planar scintigraphic imaging studies showed that this radiometal ligand has higher tumour uptake, lower background organ uptake, and higher tumour/muscle ratios than the corresponding ^{111}In-CHX-A″-DTPA conjugate, used as a reference in this study. This highlights that the structure of the chelator may significantly modify the pharmacokinetic profile of the conjugate, especially when the targeting moiety is a small peptide or molecule. Eu^{III}, Tb^{III}-BPMNTA and Gd^{III}-BPMNTA complexes are other candidates to act either as Ln^{III} luminescent probes or magnetic contrast agents, respectively. Most of Eu^{III}, Tb^{III} luminescent probes of practical use incorporate a chromophoric unit with a suitable lowest triplet-state energy level providing an efficient energy transfer to populate the Ln^{III} ion excited states (antenna effect).[14] In this direction, the photophysical properties of the 2,2'-bipyridine chromophore ($^3E_{00}$ = 23500 cm^{-1}) are favourable for an efficient antenna effect for both Eu^{III} and Tb^{III} luminescence.[15] Concerning an MRI reporter, it is well established that a Gd^{III} complex should have at least one water molecule in the inner coordination sphere of the metal allowing the proton nuclear relaxation of the lanthanide ion-bound water to be transferred to the bulk aqueous solution. Gd^{III} ion exists in aqueous solution below pH~6 as a hydrated aqua ion with ~8-9 inner-sphere water molecules. Consequently, the octadentate ligand H_5BPMNTA might leave a vacant coordination position for a water molecule.

In this contribution, the scope of H_5BPMNTA ligand is extended to the photophysical characterization of its Eu^{III} and Tb^{III} complexes together with the relaxometric properties of its Gd^{III} complex. We aim at evaluating the parameters that control luminescence and proton relaxometry in these systems (Figure 2). Moreover, we demonstrate here that a pyridine derivative of the BPMNTA chelator is suitable for its direct coupling to a $Re^{I}(bpy)(CO)_3$ core (bpy = 2,2'-bipyridine), hence affording a heterobimetallic Re^{I}/Gd^{III} complex (Figure 2). Such heterobimetallic compounds were recently reported as potential dual imaging agents allowing

simultaneous fluorescence live cell microscopy and whole body imaging.[16] Preliminary results concerning our heterobimetallic system have been published previously.[17]

Results and discussion

Synthesis

The fully protected bifunctional chelating agent **1** (Scheme 1) was synthesized according to our previously published procedures.[18] Deprotection of the two kinds ester functions (aqueous 6N HCl, 90°C) in **1** afforded pentaacid **2**, while selective deprotection of *tert*-butyl ester groups (CF_3COOH, CH_2Cl_2, rt) or methyl ester group (LiOH, THF/H_2O, rt) gave tetraacid **3** and tetraester **4**, respectively. In **4**, the carboxylic acid function can be activated *in situ* by PyBOP reagent and condensed with the amino group of 4-picolylamine, affording compound **5** in 79% isolated yield. Compound **5** was used to elaborate the heterobimetallic Re^{I}/Gd^{III} architecture (see below). On the other hand, one can note that the methyl ester function in **1** and the carboxylic acid function in **4** can be readily converted toward amine or acetylenic groups, respectively, affording other bifunctional derivatives.

The Ln^{III} (Ln = Eu, Tb, Gd) chelates derived from ligand **2** were prepared at room temperature in water solution (pH 5-6) with a slight molar excess (*ca* 10%) of the lanthanide salt ($LnCl_3 \cdot 6H_2O$) to avoid any presence of free ligand. After purification (Waters Sep-Pak column C18), the absence of free lanthanide ions was checked by the Arsenazo test[19] and no peak ascribable to the free ligand was obtained in the ESI mass spectra and HPLC analyses of these complexes. Yields were quantitative. It is noteworthy that the complexation of Ln^{III} ions by H_5BPMNTA chelator is a relatively fast reaction which is completed within an hour at room temperature, as evidenced by preliminary luminescent experiments on Eu^{III} and Tb^{III} complexes (See ESI† section, Fig. S8).

Photophysical studies of Ln-BPMNTA complexes

Investigation of the photophysical properties of the Eu- and Tb-BPMNTA complexes was carried out in Tris-buffered aqueous solutions at pH 7.4 and in various conditions. The most important photophysical parameters are gathered in Table 1. Their UV-Vis spectra are similar, displaying a strong absorption band in the low-energy region of the spectra tailing out to 340 nm (λ_{max} = 316 nm, ε > 12000 $dm^3\ mol^{-1}\ cm^{-1}$) which corresponds to $\pi \rightarrow \pi^*$ electronic transitions of the bpy core. When compared to the free ligand, the noticeable bathochromic

shift of this absorption band ($\Delta\lambda$ = 15 nm) may be associated with the *cisoid* to *transoid* isomerization of the pyridine cycles and the induced perturbation by the coordinated lanthanide ions. Photoexcitation in the lowest energy absorption band of the bpy chromophore (316 nm) was used to obtain the emission spectra of Eu^{III} and Tb^{III} complexes (Figure 3). Their emission profiles are typical of such Ln^{III} ions: five narrow bands for the Eu^{III} complex arising from the $^5D_0 \rightarrow {}^7F_J$ (J = 0 – 4) transitions are observed whereas bands arise from the $^5D_4 \rightarrow {}^7F_J$ (J = 6 – 0) transitions for the Tb^{III} complex. In these complexes, the strongest emissions are located at 617 and 544 nm, corresponding to the Eu^{III}-centred $^5D_0 \rightarrow {}^7F_2$ and Tb^{III}-centred $^5D_4 \rightarrow {}^7F_5$ hypersensitive transitions, respectively. The excitation spectra are all located within the absorption range of the ligand and have similar shapes than the absorption spectra, indicating that energy transfer from the ligand to the metal ion is operative.

For these two Eu^{III} and Tb^{III} complexes, luminescence decays are monoexponential functions, suggesting the presence of a single lanthanide coordination environment. At room temperature, the emission lifetimes of the Eu ($^5D_0$) and Tb ($^5D_4$) levels are 0.60 and 0.51 ms, respectively, that make them compatible with the use of time-resolved luminescence technique. As well reported in the literature, comparison of their lifetimes in water and deuterated water allowed us to obtain an assessment of the hydration state of these complexes (*i.e.* the number of water molecules coordinated to metal, q).[20] Thus, q values were found at 1 and 0.9 for Eu^{III} and Tb^{III} complexes, respectively. Assuming ligand BPMNTA is octadentate, these results are fitting in well with nine-coordinated Ln^{III} complexes. The calculated rate constants k_{nr}(OH) are 1200 s^{-1} (Eu complex) and 240 s^{-1} (Tb complex), signifying a contribution of 600 or 120 s^{-1} per O-H oscillator, respectively. These values are in good agreement with literature data.[21] Nevertheless, and contrary to the Eu^{III} complex, it is noteworthy that the Tb^{III} complex displays very short lifetime values at room temperature in comparison with those usually found for mono-aqua Tb^{III} complexes. Indeed, for such complexes incorporating bpy or bpy-carboxylate chromophores, lifetimes within the 1.2 – 1.5 ms (H_2O) and 2.0 - 2.5 ms (D_2O) ranges were reported.[22] These data imply the existence of an additional non-radiative pathway in the case of Tb^{III} complex, besides vibronic deactivation *via* O-H oscillators. In D_2O solution, the lifetime of the $^5D_0$ level is temperature independent between 298 K and 77 K, whereas that of the $^5D_4$ level is increased by a factor of 4.6 upon lowering the temperature at 77 K (Table 1). The corresponding high value (1350 s^{-1}) of the nonradiative temperature-dependent decay rate constant k_{nr}(T) suggests that a back energy transfer from the metal-centred level to the ligand-centred level seems to be operative in Tb-

BPMNTA. As a comparison, a $k_{nr}(T)$ value of 2100 s^{-1} was reported for a Tb-trisbipyridine cryptate in which equilibrium between chromophoric donor and Tb^{III} acceptor occurs at room temperature.[23]

To figure out whether or not such a thermally activated radiationless decay path might play a key role in the decay of the $^5D_4$-emitting state, we investigated as usual the behaviour of ligand-centred (LC) levels in the corresponding Gd^{III} complex. Room temperature Gd^{III} complex fluorescence and low-temperature Gd^{III} complex phosphorescence led us to assess that in Ln-BPMNTA complexes the singlet and triplet LC states lie at 30300 and 22100 cm^{-1}, respectively. The energy of the 0-phonon of the $^1\pi\pi^*$ LC levels was determined by the intercept of the absorption and fluorescence spectra and that of the $^3\pi\pi^*$ LC levels by the highest energy band maximum of the structured phosphorescence profile (Figure 4). The energy gap ΔE ($^1\pi\pi^*$-$^3\pi\pi^*$) amounts to 8200 cm^{-1}, predicting an efficient singlet-to-triplet intersystem crossing process.[24] We can also observe that the energy difference between the first $^3\pi\pi^*$ state of the ligand and the emissive $^5D_4$ level of terbium is around 1600 cm^{-1}. As concluded in a recent Bünzli's report, this energy gap is too low for preventing energy back-transfer onto the ligand and a concomitant loss of sensitization efficiency at room temperature.[25]

Overall quantum yields (Φ_{ov}) of these Eu^{III} and Tb^{III} complexes were determined experimentally by excitation of the ligand (λ_{exc} = 316 nm) in aerated Tris buffer at room temperature. The Φ_{ov} values are similar for both complexes (10-13%) despite the presence of a back-energy transfer observed for the Tb^{III} complex. The $\Phi_{ov}(Eu)$ value is among the largest reported in aqueous solutions for Eu^{III} complexes containing one or more 2,2'-bipyridine, while the $\Phi_{ov}(Tb)$ value lies in the medium range.[22,26] Moreover, these values are markedly higher than those reported for the mono-aqua Eu-, Tb-OCTAPA complexes, based on pyridine chromophores (Φ_{ov} < 2%).[10b] In the case of the Eu^{III} complex, it was possible to estimate the two factors which contribute to the overall quantum yield: the sensitization efficiency η_{sens} and the intrinsic luminescence quantum yield Φ_{Eu} ($\Phi_{ov} = \eta_{sens} \times \Phi_{Eu}$).[27] From experimental data (spectrum, Φ_{ov} and lifetimes) and following the methodology developed by Werts *et al.* and Beeby *et al.*,[28] the calculated values of Φ_{Eu} and η_{sens} were 13.5 and 95.5%, respectively. The value of Φ_{Eu} is comparable with other mono-hydrated Eu^{III} complexes derived from DTPA (12% - 13%)[29] and that of η_{sens} suggests that a favourable geometric effect (i.e., donor-acceptor distance) occurs in this complex. For excitation at 330 nm, the brightness ($B = \varepsilon \times \Phi_{ov}$) are 920 and 650 M^{-1} cm^{-1} for Eu^{III} and Tb^{III} complexes, respectively.

View Article Online
DOI: 10.1039/C6DT00405A

These brightness values are consistent with those required for emissive lanthanide complexes acting as tags for bioassays or optical probes.[30] Moreover, similar lifetimes and overall quantum yields of these complexes, differing in spectral output, allow their use for dual-parametric analyses.

To evaluate the potential of these Ln^{III} complexes in biological experiments, we investigated the luminescence properties of the Eu^{III} complex in buffers typically used in bioanalytical chemistry, in the presence of human serum proteins, as well as of ethylenediaminetetraacetic acid (EDTA), a strong competing ligand often used in biological experiments. The emission properties of the Eu complex as recorded in Tris buffer remained unchanged in other assessed buffers and pH range (50 mM HEPES buffer, pH 7.3; 50 mM phosphate buffer, pH 7.4 and 50 mM Borate buffer, pH 8.6). Emission spectrum, total intensity and lifetime of this complex did not differ after 24 h incubations in media containing human serum albumin (HSA) and transferrin (80 and 20 equiv., respectively). These results suggest that neither demetalation nor replacement of the innersphere water molecule by metal chelating groups lying at the surface of the proteins are occurring in the presence of an excess of these two serum protein models. Finally, the Eu complex exhibited a great resistance in presence of EDTA, a chelator which strongly binds Eu^{III} ($\log K_{Eu}$ (EDTA) = 17.32).[31] The dissociation kinetics of Eu complex was studied at room temperature (Tris buffer, pH 7.4) in presence of a 1000-fold excess of the trapping agent and by monitoring the disappearance of the $^5D_0 \rightarrow {}^7F_2$ peak at 617 nm over time. In these experimental conditions, the Eu complex was only 12% dissociated after 1.5 day. From these experiments and by using the Verhoeven analysis, $\log K_{cond}$ (pH 7.4) was found to be 19.0.[32] This value is similar to that of Gd-OCTAPA complex ($\log K_{cond}$ (pH 7.4) = 19.2), an acyclic complex containing the same donor set but in a different arrangement.[10c]

Relaxometric studies of Gd-BPMNTA complex

The ability of a Gd^{III} complex to act as a MRI contrast agent (MRI CA) is generally described in terms of its relaxivity r_1 (r_1 is the longitudinal relaxation rate enhancement induced by 1 millimole per liter of paramagnetic compound). This characteristic depends on several experimental conditions: concentration of the paramagnetic complex, magnetic field strength, temperature and pH. A 1 mM solution of Gd-BPMNTA complex at 20 MHz and neutral pH (relevant conditions to compare with MRI CA references) exhibited a relaxivity r_1 of 4.4 and 5.5 mM^{-1} s^{-1} at 310 and 298 K, respectively. This relaxivity is slightly higher than for mono-aqua Gd^{III} complexes of small size such as Gd-DTPA (3.8 mM^{-1} s^{-1} at 310 K) and Gd-

OCTAPA (5.0 mM^{-1} s^{-1} at 298 K).[10b,33] This result reflects perfectly the relationship between molecular weights of complexes and associated relaxivity values (MW = 565.6, 617.6 and 662.6 g mol^{-1} for Gd-DTPA, Gd-OCTAPA and Gd-BPMNTA, respectively). The influence of concentration and temperature on the relaxation rate of Gd-BPMNTA was also investigated at 20 MHz (See ESI† section, Figs. S14, S15). At 310 K, the study of R_1 as a function of the concentration of Gd-BPMNTA (0.5 to 3 mM) does not show any deviation from linearity, suggesting the absence of aggregates by π-stacking of the bpy moiety in solution. On the other hand, the continuous increase of the relaxivity between 318 K (r_1 = 3.6 mM^{-1} s^{-1}) and 278 K (r_1 = 8.1 mM^{-1} s^{-1}) is typical of a fast exchange between the coordinated water molecule and bulk water.

According to the Solomon-Bloembergen-Morgan theory, a set of physico-chemical (structural and dynamic) parameters of a Gd^{III} chelate, with a rather complex interplay, governs the observed r_1 values. Among them, the most relevant ones are (i) the number of water molecules (q) in the first coordination sphere of the metal, (ii) the residence time of these water molecules at the metal site (τ_M), (iii) the tumbling motion of the complex, related to its size (τ_R).[3,34]

In this relaxometry study, the number of coordinated water molecules for Gd-BPMNTA was set to one in accordance with the hydration sphere of the corresponding Eu^{III} complex (*vide supra*). At 500 MHz and within the investigated temperature range (275 – 310 K), the evolution of the bulk water transverse-relaxation rate of ^{17}O ($1/T_2^R$) for Gd-BPMNTA showed a continuous increase with decreasing temperature, indicating a maximum at lower temperature (Figure 5). This profile markedly differs from that of Gd-DTPA which exhibits a classical bell shaped curve with a maximum around 310 K. A qualitative analysis of these data suggests that Gd-BPMNTA exhibits a significantly lower value of τ_M compared to Gd-DTPA (τ_M^{310K} = 143 ns).[33] The theoretical treatment of the experimental data ($1/T_2^R$) was performed as previously described and provided a residence time of the coordinated water molecule of 3.9 ns.[35] Although the absence of maximum in the $1/T_2^R$ data may lead to some uncertainty in the calculated value, we can assume that Gd-BPMNTA exhibits a remarkably short τ_M value in comparison with those usually observed in mono-aqua gadolinium chelates.[1] Actually, this value is comparable to the τ_M reported for the TSAP isomer of a DOTA derivative (6 ns).[36] It should also be noted that this τ_M value is about three orders of magnitude shorter than that reported for the corresponding neutral bpy macrocyclic chelate.[22c] This result could be at least partly related to a more flexible coordination cage of the acyclic

View Article Online
DOI: 10.1039/C6DT00405A

complex, leading probably to a larger steric crowding around the metal ion as well as to an overall negative electric charge, another favourable factor.[37] Finally, it should be pointed out that Gd-BPMNTA τ_M value only marginally falls outside the optimal range of values (10 – 30 ns) for low imaging field (0.5 T). This is a favourable factor for molecular imaging if covalent coupling of this bifunctional chelate to a vector is considered.[38] On carrying out the fitting procedure, other parameters were calculated: hyperfine coupling constant between the ^{17}O nucleus of bound water ($A/\hbar$), activation enthalpy and entropy for the water-exchange process ($\Delta H^{\neq}$ and $\Delta S^{\neq}$, respectively), electron relaxation parameters (τ_v and B parameter) and E_v, activation energy related to τ_v. These data are reported in Table 2. The value of the $A/\hbar$ parameter is typical of what is generally observed for Gd^{III} complexes ($-3.6 \times 10^{-6} \pm 0.3$ rad s^{-1}), thus confirming the assumption of a mono-aqua complex. Besides, both the large activation enthalpy, $\Delta H^{\neq}$, and the positive activation entropy, $\Delta S^{\neq}$, point to a dissociatively activated mechanism for the water exchange, as commonly observed for nine-coordinated complexes.[39]

The ^1H NMRD profile of Gd-BPMNTA was recorded at 310 K in the proton Larmor frequency range 10 kHz – 60 MHz and compared to the NMRD profiles of Gd-DTPA and parent compound Gd-PMNTA (Figure 6).[33,11] The three complexes display the typical s-shape of low-molecular-weight and rapidly tumbling Gd^{III} chelates. Compared to Gd-DTPA, the profile of Gd-BPMNTA shows increased values over the entire investigated magnetic range as a result of its slightly higher molecular weight. The higher r_1 values observed for Gd-PMNTA (r_1 = 6.4 mM^{-1} s^{-1} at 20 MHz and 310 K) certainly arise from the higher number of Gd^{III} coordinated water molecules (q = 2 for this complex and q = 1 for the two other ones), resulting in higher relaxation. ^1H NMRD profile of Gd-BPMNTA was fitted using the usual contributions from the inner-sphere (IS) water molecules (Solomon-Bloembergen-Morgan theory) and from the outer-sphere (OS) water molecules, diffusing in the proximity of the paramagnetic complex (Freed theory).[40] In the fitting procedure some parameters were fixed: the Gd^{III}-H distance between the Gd^{III} ion and the proton nuclei of the bound water (r_{GdH} = 0.31 nm), the distance of closest approach of an outer-sphere water proton to the Gd^{III} ion (d = 0.36 nm) and the relative diffusion coefficient ($D = 2.93 \times 10^{-9}$ m^2 s^{-1}). The number of water molecules in the first coordination sphere, q, was set to 1 and the water residence time, τ_M, was fixed to the value determined by ^{17}O relaxometry. The parameters calculated from the fitting were given in Table 3, together with analogous data of other relevant Gd^{III} complexes for comparison. The tumbling rate of Gd-BPMNTA (τ_R = 76 ps) agrees with the size of the

complex and is in concordance with reference complexes data. The correlation times modulating the electronic relaxation of Gd^{III} (τ_V) are also similar while the longer electronic relaxation time at zero field (τ_{SO}) observed for Gd-PMNTA reflects its larger low-field relaxivity.

Gd-BPMNTA was also subjected to a relaxometry study for the evaluation of its possible interaction with Human Serum Albumin (HSA). At 20 MHz and 310 K, the r_1 value of the complex at a concentration of 1 mM and in the presence of 4% HSA is significantly higher than without HSA (r_1 = 6.0 *vs.* 4.4 mM^{-1} s^{-1}). Besides, the NMRD profile of the complex in the presence of HSA (Figure 7) is characterized by a hump at high fields (between 20 and 60 MHz), as observed for slowly rotating molecules. It can be assigned to the presence of a non-covalent interaction between the complex and HSA. To quantify this interaction, we used established methods involving the analysis of the paramagnetic proton relaxation rate of solutions containing 4% of HSA and various concentrations of the Gd^{III} complex at 20 MHz and 310 K (insert in Figure 7).[41] By fitting these data with equation (4) given in experimental section, we estimated a binding constant K_a of about 1170 ± 290 M^{-1} corresponding to one interaction site. Relaxivity values for free (r_1^f) and bound (r_1^b) complexes were 5.0 ± 0.5 and 10.1 ± 2.1 mM^{-1} s^{-1}, respectively. Our complex shows similar binding compared with Gd-BOPTA ($K_a = 1.5 \times 10^3$ M^{-1}), well known to interact with HSA and specifically developed as a blood agent (Multihance®, Bracco).[42] However the enhancement of the relaxivity of our HSA-bound complex with respect to the free complex is lower than anticipated (r_1^b/r_1^f = 2.0 vs. 8.2 for Gd-BOPTA). Clearly, the expected relaxation enhancement has been quenched by a direct interference of residues on protein surface in close proximity of the binding site. Luminescent experiments based on the corresponding Eu-BPMNTA complex in the presence of HSA (vide supra), suggest that a partial replacement of the metal coordinated water molecule by coordinating groups of the HSA protein does not occur. The relaxivity of the adduct is likely quenched by a decrease of the water exchange rate, despite the very short τ_M value measured for the free complex. Such a quenching has been previously observed in cases of Gd^{III} complexes with high exchange rates.[42]

Synthesis, photophysical and relaxometric properties of dinuclear Re^{I}/Gd^{III} complex (13)

As pointed out previously,[16] the association of Gd^{III} and Re^{I} cores into a heterobimetallic complex may combine MRI and optical imaging modalities in a single architecture (dual-imaging probe). Particularly, Re^{I} polypyridyl tricarbonyl complexes are generally highly luminescent, showing visible light excitation and emission, large Stokes shifts (λ_{em} - λ_{exc} > 200 nm), as well as long-emission lifetimes (µs range) which make them serious candidates for applications in cell imaging.[43] Our approach was to bind the chelating moiety (BPMNTA) as an ancillary ligand to a (bpyCOOMe)$Re^{I}(CO)_3$ core. Relying on our previous works about functionalized bpy derivatives and a dinuclear $Re^{I}/^{99m}Tc$ complex, the incorporation of an aromatic ester functionality on the bpy unit of the Re^{I} core seemed a relevant way for subsequent bioconjugation.[18,44]

Scheme **2** outlines the followed preparative strategy for accessing to the heterodinuclear Re^{I}/Gd^{III} complex **13**. The new Re^{I} complexes **9** and **10** were obtained through a classical pathway involving preparation of the (bpy-COOMe)$Re(CO)_3Cl$ complex by reacting 4-carbomethoxy-2,2'-bipyridine with a slight excess of the $Re(CO)_5Cl$ precursor in refluxing methanol (1.2:1 metal:ligand ratio) and its further activation with triflate silver salts in acetonitrile. The reactive intermediate CH_3CN adduct **10** was readily obtained in excellent yield (91% for the two steps) by using simple filtration and recrystallization procedures. Under microwave irradiation (155 W at 105°C in THF), the substitution of the Re-bound acetonitrile molecule of **10** by the ancillary pyridinic ligand **5** took place within 1 h, thus affording the desired complex **11** in 56% yield after purification by column chromatography on alumina. It is worth noting that by using classical thermal activation ($NaHCO_3$, CH_3CN, reflux, overnight), complex **11** was obtained in 40% isolated yield. Selective deprotection of *tert*-butyl groups was performed in acidic conditions (CF_3COOH) at room temperature and the subsequent treatment of the tetraacid compound **12** with $GdCl_3$ in water yielded the neutral heterodinuclear complex **13**. All complexes display metal carbonyl stretching frequencies in the range 2050-1880 cm^{-1} which are consistent with a facial (*fac*) isomer arrangement at the rhenium centre. The single and strong IR absorption at ~ 2030 cm^{-1} can be assigned to the axial C≡O group, whereas equatorial carbonyl ligands gave IR absorption in the 1930-1900 cm^{-1} range, with a broad and intense band which splits into two peaks in the case of complex **9**. In ^{13}C NMR spectra, three signals assigned to C≡O groups were also observed in the 190-195 ppm range. In addition, ^{1}H, ^{13}C NMR, UV-Vis and emission spectra of the complexes provided evidence of the presence of the bpy and pyridine ligands within the

Re^{I} coordination sphere while their MS spectra gave isotopic distribution in agreement with the proposed structures.

The UV-Vis absorption and emission spectra of complexes **9**-**13** were recorded at room temperature and in aerated CH_3CN or aqueous solution (Tris buffer, pH 7.4). Relevant photophysical data are given in Table 4. Unfortunately, the luminescence lifetime of these complexes (τ < 30 μs) could not be measured due to instrumental limitations. The electronic spectra of these Re^{I} species showed the typical characteristics of bis-imine Re^{I} derivatives displaying several absorption bands in the 240 – 450 nm range. The two bands at high energies (λ < 320 nm) with high extinction coefficients ($\varepsilon > 10^4$ dm^3 mol^{-1} cm^{-1}) are assigned to intraligand (IL) transitions of the appended chromophores [π→π* (bpyCOOMe and py-bpy)]. On the basis of previous spectroscopic studies of Re^{I}(bpy)tricarbonyl complexes,[43c,45] the lower-energy absorption band (340-450 nm) with extinction coefficient in the order of 10^3 dm^3 mol^{-1} cm^{-1} is associated to spin-allowed metal-to-ligand charge-transfer (^{1}MLCT, formally, Re(dπ-bpyCOOMe (π*)). For all complexes, excitation into the ^{1}MLCT absorption band leads to a broad structureless emission band extending from 500 to 800 nm. This emission band remains unchanged with the energy of excitation and is typical of the phosphorescence derived from the triplet rhenium-to-ligand charge transfer (^{3}MLCT) excited state. By comparison with (bpy)$Re^{I}(CO)_3Cl$ or (bpy)$Re^{I}(CO)_3CH_3CN$ complexes, substitution of the bpy moiety by an electron withdrawing group in **9** and **10** leads to a red-shift for both ^{1}MLCT absorption and ^{3}MLCT emission bands.[46] On the other hand, the coordination of the BPMNTA moiety to Gd^{III} induces in **13** a red-shift (13 nm) of the lowest energy of intraligand transition but does not significantly influence both ^{1}MLCT absorption and ^{3}MLCT emission bands as well as the emission quantum yield of the Re^{I} core (Figure 8). Compared to its precursor complex **12**, the lack of quenching associated to the Re ^{3}MLCT state in complex **13** is expected. Actually, the Gd^{III} excited levels have far higher energies (> 31000 cm^{-1}) than those of Re chromophore MLCT states, thus preventing any Re → Gd energy transfer process. As far as the target dinuclear complex **13** is concerned, it was characterized by a ^{1}MLCT absorption band at 367 nm, a ^{3}MLCT emission band with a maximum at 588 nm and an emission quantum yield of 1.4%. Although this latter value is rather low, it is large enough for detection in fluorescence microscopy.[47] Moreover, the emission intensity of the ^{3}MLCT band of **13** remained unchanged over a two-day period in Tris buffer (pH 7.4), in presence of 200 molecular excess of histidine (a strong competing ligand for a Re^{I} core), EDTA (1000 equiv.) or in a Tris buffer/serum (2/1) mixture.

The Re^{I}/Gd^{III} complex was subsequently investigated for its relaxometric properties, by assessment of relaxivity values r_1, by analysis of the temperature dependence of the reduced transverse relaxation rate of ^{17}O and by recording the NMRD profile at 310 K (Figure 9) in order to estimate the r_1, τ_M and τ_R key parameters. Theoretical treatments of these experimental data were performed as mentioned before by using the IS and OS model, assuming the presence of a mono-aqua Gd-BPMNTA core (See ESI† section, Tables S1 and S2). At 310 K, the experimental r_1 values were 6.6 mM^{-1} s^{-1} at 20 MHz and 6.0 mM^{-1} s^{-1} at 60 MHz, *i.e.* significantly higher than those of Gd-BPMNTA parent complex. As observed for Gd-BPMNTA, the influence of concentration and temperature on dinuclear complex suggests the lack of aggregates and no limitation of relaxivity by the water residence time. We note also a similar ^{17}O NMR profile than for Gd-PMNTA, with a maximum of the curve located at a temperature lower than 275 K. As expected, the theoretical analysis of the ^{17}O NMR data provides a short residence time of the coordinated water molecule (τ_M = 9.0 ns) in accordance with what was observed for the Gd-BPMNTA complex (τ_M = 3.9 ns). The presence of the extra Re^{I} core poorly influences the value of the exchange rate, as expected for moieties that do not contribute to the coordination sphere of Gd^{III} ion. The NMRD profile of **13** had the typical shape for a low-molecular weight complex, with no hump observed at high magnetic fields (20 – 60 MHz) and revealed a higher relaxivity at all magnetic fields compared to Gd-BPMNTA complex. This improved relaxivity is due to a slower tumbling rate as evidenced by a higher calculated τ_R value (138 ps) than for Gd-BPMNTA (76 ps). This is in good agreement with the increase by a factor 1.9 of the dinuclear complex molecular weight. In order to compare with Gd-BPMNTA, the interaction of **13** with HSA was also investigated. At 20 MHz and 310 K, the r_1 relaxivity value of **13** in the presence of 4% HSA is 7.4 mM^{-1} s^{-1}, corresponding to an enhancement of 12% without HSA. The slight increase of the longitudinal apparent relaxivity is minimal and can be rather explained by an increase in the viscosity of medium compared to water solution than by a specific interaction between **13** and HSA. This result is promising, because a molecular imaging agent must specifically bind to its target and avoid non-specific interferences with blood macromolecules such HSA.

Conclusions

The mono-aqua Ln^{III} complexes (Ln = Eu, Tb, Gd) of the bifunctional chelating agent H_5BPMNTA show promising photophysical and relaxometric properties. In aqueous media,

the Eu^{III} complex displays an emission lifetime of 0.60 ms at room temperature and an overall quantum yield of 12.9% under an excitation at 316 nm. The Tb^{III} complex displays similar lifetime and quantum yield values despite the presence of a back energy transfer process ($^5D_4$ Tb $\rightarrow {}^3\pi\pi^*$ ligand) according to the energy-gap law ($E(^3\pi\pi^*) - E(^5D_4)$). These complexes are also characterized by a good kinetic stability both in aqueous buffers generally used in bioanalytical analyses and in media containing blood proteins. The Gd^{III} complex shows a r_1 relaxivity at the upper limit of values observed for clinically used MRI contrast agents combined to a much more appealing water residence time (τ_M = 3.9 ns), optimum for vectorisation. In addition, we demonstrate that a pyridinic derivative of H_5BPMNTA can self-assemble with a (bpy)$Re^I(CO)_3$ core, giving rise to a neutral heterobimetallic Re^I/Gd^{III} complex, highly soluble and stable in aqueous solution. This dinuclear complex leads to an increase of the τ_R rotational tumbling time of the Gd-BPMNTA core, resulting in an enhancement of the r_1 relaxivity by a factor of 1.5. In addition, it exhibits orange broad-band emission upon excitation in the visible range (367 nm) with a quantum yield of 1.4% in aqueous solution, sufficiently large for detection in fluorescence microscopy. Finally, a significant binding of Gd-BPMNTA complex with HSA was observed, but none with the dinuclear Re^I/Gd^{III} complex. Taking into account both the luminescent and relaxometric properties of Ln-BPMNTA complexes and our previous work on ^{111}In-BPMNTA radiocomplex,[13] H_5BPMNTA ligand can be further explored as an efficient platform to get probes for a multimodal imaging purpose. Moreover, the presence of a reactive function in the BPMNTA core offers an interesting opportunity for the construction of heteropolymetallic complexes and conjugation to biomolecules or nanomaterials.

Experimental

General

Reactions utilizing microwave technology were conducted in a CEM Discover Benchmate microwave reactor (model nr.908010). ^{1}H and ^{13}C spectra were recorded on Bruker Avance 300, 400 and 500 working at 300, 400 and 500 MHz respectively. For ^{1}H chemical shifts (δ) are given in ppm relative to a residual protiated solvent and coupling constants (J) are given in Hertz. IR spectra were recorded on a Perkin-Elmer FT-IR 1725x spectrometer using KBr pellets (solid samples) and NaCl plates (liquid samples). Electrospray (ES) mass spectra were obtained on a Q TRAP Applied Biosystems spectrometer and High-Resolution Mass Spectra

View Article Online
DOI: 10.1039/C6DT00405A

(HRMS) on a Xevo G2 QTof Waters spectrometer. DCI mass spectra were obtained on a DSQ II Thermo Fisher. Elemental analyses were carried out by the "Service d'Analyse", Laboratoire de Chimie de Coordination (Toulouse). The analytical HPLC analyses were performed on a Waters Alliance 2695 system with a PDA 2996 detector and using a reverse-phase column (Phenomenex Luna C8, 5 µm, 100 Å, 150 x 4.6 mm) with a flow rate of 1 mL/min. Linear gradient system was $HCOONH_4$ 10 mM pH 4/CH_3CN 100/0 to 80/20 in 18 min (system A) or 90/10 to 10/90 in 18 min (system B). The analytical UPLC analyses were performed on a Acquity UPLC Waters system with a PDA detector and using a reverse phase column (Acquity BEH C18 column, 1.7 µm, 100 Å, 50 x 2.1 mm) with a flow rate of 0.6 mL/min. Linear gradient system was $HCOONH_4$ 10 mM pH 4/CH_3CN + 10% $HCOONH_4$ 100 mM pH 4 80/20 to 0/100 in 7 min

Pentaester compound **1** was synthesized according to our previously published procedures.[18]

Photophysical measurements

Absorption measurements were done with a Hewlett Packard 8453 temperature-controlled spectrometer in 10 mm quartz cuvette. Fluorescence spectra at room temperature were obtained using a Cary Eclipse spectrofluorimeter equipped with a Xenon flash lamp source and a Hamamatsu R928 photomultiplier tube. The measurements were carried out at pH 7.4 in Tris buffer (50 mM) or CH_3CN and all samples were prepared with an absorbance between 0.01 and 0.05 at the excitation wavelength in order to prevent the inner-filter effect. Phosphorescence spectra at 77 K were recorded with a LS-50B Perkin-Elmer spectrofluorimeter equipped with a Xenon flash lamp source, a Hamamatsu R928 photomultiplier tube and the low-temperature accessory No. L2250136. Lifetimes τ (uncertainty ≤ 5%) were measured by monitoring the decay at a wavelength corresponding to the maximum intensity of the emission spectrum, following pulsed excitation. They are the average values from at least five separate measurements covering two or more lifetimes. The luminescence decay curves were fitted by an equation of the form $I(t) = I(0) \exp(-t/\tau)$ by using a curve-fitting program. High correlation coefficients were observed in each cases (higher than 0.999). The luminescence quantum yields (uncertainty ± 15%) were determined by the method described by Haas and Stein [48] using as standards $[Ru(bpy)_3]^{2+}$ in aerated water ($\Phi = 0.04$)[49] for the Eu(III) and Re(I) complexes or quinine sulfate in 1N sulfuric acid ($\Phi = 0.546$)[50] for the Tb(III) complex and corrected for the refractive index of the solvent. They

View Article Online
DOI: 10.1039/C6DT00405A

were measured according to conventional procedures with diluted solutions (optical density < 0.05).

The sensitization efficiency η_{sens} and the intrinsic luminescence quantum yield Φ_{Eu} were calculated by using the following equations:[28]

$$\eta_{sens} = \Phi_{ov} / \Phi_{Eu} \quad (1)$$

$$\Phi_{Eu} = \tau_{obs} / \tau_R \quad (2)$$

$$1 / \tau_R = k_r = 14.65 \times n^3 \times (I_{\Sigma Fj} / I_{F1}) \quad (3)$$

where τ_{obs} is the observed lifetime, τ_R the radiative lifetime, $I_{\Sigma Fj}$ the integrated intensity of the entire emission spectrum, I_{F1} the integrated intensity of the purely magnetic dipole transition $^5D_0 \rightarrow {}^7F_1$ and n the refractive index of the solution.

NMR measurements

Proton nuclear magnetic relaxation dispersion (NMRD) profiles were recorded on a Stelar Spin fast field cycling (FFC) NMR relaxometer (Mede, Italy) working between 0.24 mT and 1 T. The measurements were performed at 310 K with samples (0.6 mL) in 10 mm o.d. Pyrex tubes. The additional relaxation rates at 0.47 and 1.41 T were measured on mq-20 and mq-60 Minispec systems (Bruker, Karlsruhe, Germany), respectively. Fitting of the ^{1}H NMRD was performed with data-processing software using different theoretical models describing the nuclear-relaxation phenomena observed (Minuit, CERN Library).[51,52] The exact Gd^{3+} concentration was determined by proton relaxivity measurements at 0.47 T and 37 °C after complete hydrolysis in concentrated HNO_3.

^{17}O NMR measurements of solutions were performed at 11.75 T on 0.35 mL samples contained in 5 mm o.d. tubes on a Bruker Avance 500 spectrometer. The temperature was regulated by air or nitrogen flow controlled by a Bruker BVT 3200 unit.

^{17}O diamagnetic transverse-relaxation times of water were measured using the Carr-Purcell-Meiboom-Gill (CPMG) sequence (90° and 180° pulse lengths were 25 and 50 µs, respectively). All ^{17}O NMR spectra were proton decoupled. ^{17}O transverse-relaxation times of water in solutions containing the Gd complex were calculated from the spectral line width. The data are presented as the reduced transverse relaxation rate ($1/T_2^R = 55.55/(q \times [complex] \times 1/T_2^p$) where q is the number of inner-sphere water molecules, [complex] is the molar concentration of the Gd complex and T_2^p is the paramagnetic transverse relaxation rate.

For the study of noncovalent interaction with HSA, the proton paramagnetic relaxation rate data (R_1^p) were obtained at fixed field strength (0.47 T) and temperature (310 K) using a

Minispec mq-20 (Bruker, Karlsruhe, Germany). The HSA concentration was set to 0.6 mM (4%) and the concentration of the Gd^{III} agent ranged from 0 to 1.5 mM.

The proton data obtained in HSA solution were fitted using equation (4):[41]

$$R_1^p = 1000 \times\{(r_1^f \times L_0) + 0.5\times(r_1^b - r_1^f) \times [(N\times P_0) + L_o + K_a^{-1} - \sqrt{[(N\times P_0) + L_0 + K_a^{-1})^2 - 4\times N\times L_0\times P_0]]\}} \quad (4)$$

where K_a is the association constant, P_0 is the protein concentration, L_0 is the concentration of the paramagnetic complex, N is the number of independent and identical interaction sites, and r_1^b and r_1^f (mM^{-1} s^{-1}) are the relaxivities of the HSA–contrast agent adduct and the free contrast agent, respectively.

2,2′,2″,2‴-[(4-carboxy-2,2′-bipyridine-6,6′-diyl)bis(methylenenitrilo)]-tetrakis (acetic acid) (2). The pentaester **1** (590 mg, 0.81 mmol) was stirred in a 6M HCl solution (30 mL) at 90 °C for 4 days. After cooling to room temperature, the solution was washed with diethylether (20 mL), and the aqueous layer was evaporated under reduced pressure to give **2** in the form of its trishydrochloride salt as a white solid (515 mg, 100%). IR ν/cm^{-1} 3385, 3185, 3009, 1723br, 1591, 1572, 1510. ^{1}H NMR (300 MHz; DMSO-d_6): δ3.53 (s, 4H), 3.55 (s, 4H), 4.08 (s, 2H), 4.13 (s, 2H), 7.65 (dd, J = 7.7, 1.1 Hz, 1H), 7.96 (t, J = 7.7 Hz, 1H), 8.05 (d, J = 1.5 Hz, 1H), 8.26 (dd, J = 7.7, 1.1 Hz, 1H), 8.66 (d, J = 1.5 Hz, 1H), 12.60 (br s, 4H). ^{13} C NMR (75 MHz; DMSO-d_6): δ 54.3 (CH_2), 54.4 (CH_2), 59.1 (CH_2), 59.5 (CH_2), 118.0 (CH), 119.1 (CH), 122.1 (CH), 123.4 (CH), 137.9 (CH), 140.0 (Cq), 153.8 (Cq), 155.6 (Cq), 159.2 (Cq), 160.3 (Cq), 166.4 (CO), 172.4 (CO), 172.45 (CO). ES^+/MS: m/z 491.4 ($[M+H]^+$, 100%), 513.4 ($[M+Na]^+$, 75%), 529.3 ($[M+K]^+$, 65%). ES^+/HRMS Calcd for $C_{21}H_{23}N_4O_{10}$ $[M+H]^+$: m/z = 491.1414, found: m/z = 491.1421. UV/Vis λ_{max} (50 mM Tris buffer, pH 7.4)/nm: 238 (ε/dm^3 mol^{-1} cm^{-1} 9000), 301 (8800). Anal. Found: C, 39.37; H, 4.64; N, 8.74. Calcd for $C_{21}H_{22}N_4O_{10}\cdot 3HCl\cdot 2H_2O$: C, 39.67; H, 4.60; N, 8.81.

Ln-BPMNTA chelates. General procedure: To a solution of compound **2** in H_2O was added $LnCl_3$,$6H_2O$ (1.1 equiv.). After stirring at room temperature for 1h, pH was adjusted to 5-6 with NaOH 0.1M and the mixture was then stirred overnight at room temperature. The solvent was evaporated to a minimum and the solution was loaded on a Waters Sep-Pak column (C_{18}, 10 g). Column was rinsed with 5x8 mL of H_2O to remove salts and the product was eluted

with a H_2O/MeOH mixture (1/1, 5x1 mL). The solvents were removed *in vacuo* to give the expected complexes with quantitative yields. The absence of free Ln(III) ion in these complexes was verified using a classic test with an arsenazo indicator solution.

Eu-BPMNTA complex. HPLC analysis (system A); t_R = 4.7 min. ES$^-$/MS: *m/z* 639.2 ([M-2Na+H]$^-$, 100%). UV/Vis λ_{max} (50 mM Tris buffer, pH 7.4)/nm: 246 (ε/dm^3 mol^{-1} cm^{-1}10500), 316 (12200). Luminescence λ_{em} (50 mM Tris buffer, pH 7.4; λ_{exc} = 316 nm)/nm: 580 (relative intensity, corrected spectrum 2), 592 (32), 617 (100), 652 (5), 676-714 (70).

Tb-BPMNTA complex. HPLC analysis (system A); t_R = 4.7 min. ES$^-$/MS: *m/z* 645.2 ([M-2Na+H]$^-$, 100%). UV/Vis λ_{max} (50 mM Tris buffer, pH 7.4)/nm: 246 (ε/dm^3 mol^{-1} cm^{-1} 9600), 316 (12100). Luminescence λ_{em} (50 mM Tris buffer, pH 7.4; λ_{exc} = 316 nm)/nm: 490 (relative intensity, corrected spectrum 43), 544 (100), 584 (33), 623 (15), 636-693 (7).

Gd-BPMNTA complex. HPLC analysis (system A); t_R = 4.7 min. ES$^-$/MS: *m/z* 644.0 ([M-2Na+H]$^-$, 100%). ES$^-$/HRMS Calcd for $C_{21}H_{18}N_4O_{10}Gd$ [M-2Na+H]$^-$: *m/z* = 644.0269, found: *m/z* = 644.0265. UV/Vis λ_{max} (50 mM Tris buffer, pH 7.4)/nm: 246 (ε/dm^3 mol^{-1} cm^{-1} 9900), 316 (12100).

2,2′,2″,2‴-{[4-(methoxycarbonyl)-2,2′-bipyridine-6,6′-diyl]bis(methylenenitrilo)}-tetrakis (acetic acid) (3). To a solution of pentaester **1** (175 mg, 0.24 mmol) in CH_2Cl_2 (7 mL) was added 7 mL of CF_3CO_2H, and the resulting solution was stirred at rt for 18 h. The reaction mixture was evaporated to dryness, and the residue was taken up in 2 mL of MeOH. 14 mL of Et_2O were added, resulting in the precipitation of a fine white solid, which was collected by filtration, washed with Et_2O, and dried, to yield tetraacid **3** as a pale grey solid (105 mg, 87%). mp ≈ 180 ºC (dec.). IR ν/cm^{-1} 3436, 1728, 1635, 1405. ^{1}H NMR (300 MHz; DMSO-d_6): δ 3.53 (s, 8H), 3.94 (s, 3H), 4.08 (s, 2H), 4.13 (s, 2H), 7.64 (d, *J* = 6.8 Hz, 1H), 7.96 (m, 1H), 8.07 (s, 1H), 8.27 (d, *J* = 6.5 Hz, 1H), 8.66 (s, 1H). ^{13}C NMR (75 MHz; DMSO-d_6): δ 52.8 (CH_3), 54.35 (CH_2), 54.4 (CH_2), 59.0 (CH_2), 59.3 (CH_2), 117.6 (CH), 119.1 (CH), 121.8 (CH), 123.4 (CH), 137.9 (CH), 138.6 (Cq), 153.5 (Cq), 155.6 (Cq), 159.1 (Cq), 160.5 (Cq), 165.3 (CO), 172.4 (CO). ES$^+$/MS: *m/z* 505.1 ([M+H]$^+$, 100%). ES$^-$/HRMS Calcd for $C_{22}H_{23}N_4O_{10}$ [M-H]$^-$: *m/z* = 503.1414, found: *m/z* = 503.1418.

Tetra (*tert*-butyl) 2,2′,2″,2‴-[(4-carboxy-2,2′-bipyridine-6,6′-diyl)bis(methylenenitrilo)]-tetrakis (acetate) (4). To a solution of pentaester **1** (59 mg, 0.08 mmol) in THF (1 mL) was

View Article Online
DOI: 10.1039/C6DT00405A

added lithium hydroxide monohydrate (4 mg, 0.09 mmol) in H_2O (1 mL). The mixture was vigorously stirred at rt for 2 h and then H_2O (10 mL) and CH_2Cl_2 (10 mL) were added. The pH of the aqueous phase was adjusted to 6 with HCl 1M. The organic phase was dried ($MgSO_4$) and the solvent was removed under reduced pressure. The crude product was purified by chromatography over silica gel (CH_2Cl_2/MeOH 97:3) to give tetraester **4** as a colourless oil (51 mg, 89%). R_f (silicagel, CH_2Cl_2/MeOH 90:10): 0.3. IR ν/cm^{-1} 2978, 2931, 1732, 1613, 1574, 1456. ^{1}H NMR (300 MHz; $CDCl_3$): δ 1.39 (s, 18H), 1.40 (s, 18H), 3.39 (s, 4H), 3.47 (s, 4H), 3.92 (s, 2H), 4.07 (s, 2H), 7.20 (d, J = 7.5 Hz, 1H), 7.76 (t, J = 7.7 Hz, 1H), 7.89 (s, 1H), 7.96 (d, J = 7.7 Hz, 1H), 8.50 (s, 1H). ^{13}C NMR (75 MHz; $CDCl_3$): δ 28.0 (CH_3), 56.6 (CH_2), 57.0 (CH_2), 60.2 (CH_2), 60.7 (CH_2), 82.1 (Cq), 82.2 (Cq), 120.5 (CH), 121.0 (CH), 122.8 (CH), 124.0 (CH), 138.2 (CH), 151.2 (Cq), 153.9 (Cq), 155.8 (Cq), 156.1 (Cq), 156.7 (Cq), 168.6 (CO), 171.0 (CO), 171.4 (CO). ES$^+$/MS: m/z 715.6 ([M+H]$^+$, 100%), 737.6 ([M+Na]$^+$, 15%). ES$^+$/HRMS Calcd for $C_{37}H_{55}N_4O_{10}$ [M+H]$^+$: m/z = 715.3918, found: m/z = 715.3928.

Tetra (*tert*-butyl) 2,2′,2″,2‴-{[4-(pyridin-4-ylmethylcarbamoyl)-2,2′-bipyridine-6,6′-diyl]bis(methylenenitrilo)}-tetrakis (acetate) (5). To a solution of carboxylic acid compound **4** (230 mg, 0.322 mmol) in CH_2Cl_2 (18 mL) were added PyBoP (276 mg, 0.530 mmol), *N*,*N*-diisopropylethylamine (208 mg, 1.61 mmol) and 4-(aminomethyl)pyridine (45.3 mg, 0.419 mmol). The mixture was stirred at rt for 48 h, washed with 0.1N HCl aqueous solution (3 × 5 mL), then 0.1N NaOH aqueous solution (3 × 5 mL) and water (3 × 5 mL). The organic layer was dried over $MgSO_4$ and evaporated under reduced pressure. The oily residue was purified by column chromatography over alumina (petroleum ether/ethyl acetate 70:30) to give **5** as a white solid (204 mg, 79%). UPLC analysis: t_r = 4.93 min. ^{1}H NMR (300 MHz; $CDCl_3$): δ 1.36 (s, 36H), 3.44 (s, 8H), 4.00 (s, 2H), 4.10 (s, 2H), 4.62 (d, J = 5.9 Hz, 2H), 7.21 (d, J = 6.0 Hz, 2H), 7.47 (dd, J = 7.8, 0.5 Hz, 1H), 7.71 (t, J = 7.8 Hz, 1H), 8.07 (d, J = 1.4 Hz, 1H), 8.13 (t, J = 5.9 Hz, 1H), 8.24 (dd, J = 7.8, 0.5 Hz, 1H), 8.43 (d, J = 6.0 Hz, 2H), 8.71 (d, J = 1.4 Hz, 1H). ^{13}C NMR (75 MHz; $CDCl_3$): δ 27.93 (CH_3), 27.94 (CH_3), 42.5 (CH_2), 55.74 (CH_2), 55.77 (CH_2), 59.1 (CH_2), 59.6 (CH_2), 80.9 (Cq), 81.0 (Cq), 116.6 (CH), 119.4 (CH), 120.7 (CH), 122.3 (CH), 123.4 (CH), 137.3 (CH), 142.2 (Cq), 147.4 (Cq), 149.5 (CH), 154.5 (Cq), 156.2 (Cq), 157.8 (Cq), 159.8 (Cq), 165.9 (CO), 170.4 (CO), 170.6 (CO). ES$^+$/MS: m/z 805.5 ([M+H]$^+$, 100%), 827.5 ([M+Na]$^+$, 15%). ES$^+$/HRMS Calcd for $C_{43}H_{61}N_6O_9$ [M+H]$^+$: m/z = 805.4500, found: m/z = 805.4509; Calcd for $C_{43}H_{60}N_6O_9Na$ [M+Na]$^+$: m/z = 827.4319, found:

View Article Online
DOI: 10.1039/C6DT00405A

m/z = 827.4327. Anal. Found: C, 63.91; H, 7.47; N, 10.12. Calcd for $C_{43}H_{60}N_6O_9$: C, 64.16; H, 7.51; N, 10.44.

Tetra (*tert*-butyl) 2,2′,2″,2‴-{[4-(but-3-yn-1-ylcarbamoyl)-2,2′-bipyridine-6,6′-diyl]bis(methylenenitrilo)} -tetrakis (acetate) (6). To a stirred solution of carboxylic acid compound **4** (260 mg, 0.364 mmol) and but-3-yn-1-amine hydrochloride[53] (50 mg, 0.476 mmol) in CH_2Cl_2 (20 mL) were added, at rt under argon, diisopropylethylamine (236 mg, 1.83 mmol) and PyBOP (312 mg, 0.600 mmol). The resulting solution was stirred at rt for 24 h, then sequentially washed with aq. HCl 0.1M (3×20 mL), aq. NaOH 1M (2×20 mL) and H_2O (20 mL). The organic layer was dried (Na_2SO_4), and the solvent was removed under reduced pressure. The crude product was purified by flash chromatography over alumina (petroleum ether/ethylacetate 70:30), to give the corresponding acetylenic compound (200 mg, 72%) as a colorless oil. ^{1}H NMR (300 MHz; $CDCl_3$): δ 1.46 (s, 18H), 1.47 (s, 18H), 2.06 (t, *J* = 2.6 Hz, 1H), 2.56 (td, *J* = 6.8, 2.6 Hz, 2H), 3.52 (s, 8H), 3.65 (q, *J* = 6.0 Hz, 2H), 4.11 (s, 2H), 4.17 (s, 2H), 7.39 (t, *J* = 5.9 Hz, 1H), 7.57 (dd, *J* = 7.7, 1.1 Hz, 1H), 7.78 (t, *J* = 7.7 Hz, 1H), 8.05 (d, *J* = 1.6 Hz, 1H), 8.31 (dd, *J* = 7.8, 1.1 Hz, 1H), 8.69 (d, *J* = 1.6 Hz, 1H). ^{13}C NMR (75 MHz; $CDCl_3$): δ 19.5 (CH_2), 28.26 (CH_3), 28.29 (CH_3), 38.9 (CH_2), 55.97 (CH_2), 56.03 (CH_2), 59.6 (CH_2), 59.8 (CH_2), 70.2 (CH), 81.2 (Cq), 81.3 (Cq), 81.5 (Cq), 116.8 (CH), 119.7 (CH), 120.8 (CH), 123.6 (CH), 137.6 (CH), 143.1 (Cq), 154.9 (Cq), 156.5 (Cq), 158.3 (Cq), 160.0 (Cq), 166.1 (CO), 170.7 (CO), 170.8 (CO). ES$^+$/MS: *m/z* 766.2 ([M+H]$^+$, 20%), 788.1 ([M+Na]$^+$, 100%).

Tetra (*tert*-butyl) 2,2′,2″,2‴-{[4-(-2-aminoethylcarbamoyl)-2,2′-bipyridine-6,6′-diyl]bis(methylenenitrilo)} -tetrakis (acetate) (7). To ethylenediamine (140 mg, 2.33 mmol) was added pentaester **1** (52 mg, 0.071 mmol) and the mixture was stirred at rt for 24 h. Elimination of diamine under reduced pressure afforded compound **7** as a tan oil (53 mg, 100%). IR ν/cm^{-1} 3364, 3300, 3065, 2978, 2932, 1733, 1661, 1558. ^{1}H NMR (300 MHz; $CDCl_3$): δ 1.43 (s, 36H), 2.94 (m, 3H), 3.48 (s, 4H), 3.49 (s, 4H), 3.54 (m, 2H), 4.09 (s, 2H), 4.13 (s, 2H), 7.51 (d, *J* = 7.7 Hz, 1H), 7.75 (t, *J* = 7.7 Hz, 1H), 8.05 (s ,1H), 8.28 (d, *J* = 7.7Hz, 1H), 8.70 (s, 1H). ^{13}C NMR (75 MHz; $CDCl_3$): δ 28.10 (CH_3), 28.15 (CH_3), 41.4 (CH_2), 42.9 (CH_2), 55.7 (CH_2), 55.9 (CH_2), 59.5 (CH_2), 59.7 (CH_2), 81.1 (Cq), 81.2 (Cq), 116.9 (CH), 119.7 (CH), 120.8 (CH), 123.5 (CH), 137.4 (CH), 143.1 (Cq), 155.0 (Cq), 156.2 (Cq), 158.1 (Cq), 159.7 (Cq), 166.2 (CO), 170.6 (CO), 170.7 (CO). ES$^+$/MS: *m/z* 757.8 ([M+H]$^+$, 100%),

View Article Online
DOI: 10.1039/C6DT00405A

779.8 ([M+Na]$^+$, 72%). ES$^+$/HRMS Calcd for $C_{39}H_{61}N_6O_9$ [M+H]$^+$: m/z = 757.4500, found: m/z = 757.4503.

4-Carbomethoxy-2,2'-bipyridine (8). To a solution of methyl 2-bromopyridine-4-carboxylate (317 mg, 1.47 mmol) in anhydrous toluene (15 mL) were added $Pd(PPh_3)_4$ (342 mg, 0.30 mmol), CuBr (34 mg, 0.24 mmol) and 2-(tributylstannyl)pyridine (654 mg, 1.78 mmol). The reaction mixture was then degassed *in vacuo* and heated at 140°C under microwave irradiation (260 W) for 2 hours. The solution was filtered through a pad of Celite, concentrated and loaded on a alumina column (eluent: petroleum ether/CH_2Cl_2 50:50) to provide **8** as a white solid (227 mg, 72%). mp 82-83°C. R_f (alumina, petroleum ether/CH_2Cl_2 50:50): 0.38. IR ν/cm^{-1} 1723. ^{1}H NMR (300 MHz; $CDCl_3$): δ 3.99 (s, 3H), 7.34 (ddd, J = 1.2, 4.8, 7.5 Hz, 1H), 7.84 (td, J = 1.6, 8.0 Hz, 1H), 7.86 (dd, J = 1.6, 5.0 Hz, 1H), 8.42 (td, J = 1.0, 8.0 Hz, 1H), 8.72 (ddd, J = 0.9, 1.8, 4.8 Hz, 1H), 8.82 (dd, J = 0.8, 5.0 Hz, 1H), 8.94 (dd, J = 0.9, 1.6 Hz, 1H). ^{13}C NMR (75 MHz; $CDCl_3$): δ 52.6 (CH_3), 120.4 (CH), 121.2 (CH), 122.8 (CH), 124.1 (CH), 137.1 (CH), 138.4 (Cq), 149.3 (CH), 149.9 (CH), 155.3 (Cq), 157.3 (Cq), 165.7 (CO).

(bpy-COOMe)Re(CO)$_3$Cl (9). To a solution of **8** (50 mg, 0.233 mmol) in MeOH (10 mL) was added $Re(CO)_5Cl$ (101.3 mg, 0.28 mmol) and the reaction mixture was refluxed overnight at 65°C. After cooling down to room temperature, the solvent was evaporated to the third and the resulting precipitate was filtered and washed with cold MeOH to obtain **9** as a yellow solid (110 mg, 91%). IR ν/cm^{-1} 2018, 1914, 1877, 1729. ^{1}H NMR (300 MHz; $CDCl_3$): δ 4.07 (s, 3H), 7.60 (ddd, J = 1.3, 5.5, 7.7 Hz, 1H), 8.04 (dd, J = 1.6, 5.7 Hz, 1H), 8.13 (ddd, J = 1.6, 7.7, 8.2 Hz, 1H), 8.34 (ddd, J = 0.7, 1.2, 8.3 Hz, 1H), 8.73 (dd, J = 0.8, 1.7 Hz, 1H), 9.09 (ddd, J = 0.8, 1.6, 5.5 Hz, 1H), 9.21 (dd, J = 0.8, 5.7 Hz, 1H). ^{13}C NMR (125 MHz; $CDCl_3$): δ 53.7 (CH_3), 122.6 (CH), 123.6 (CH), 126.2 (CH), 127.6 (CH), 139.1 (CH), 139.8 (Cq), 153.3 (CH), 154.0 (CH), 155.0 (Cq), 156.8 (Cq), 163.4 (C=O), 188.8 (C≡O), 196.7 (C≡O), 196.8 (C≡O). DCI-NH_3/MS: m/z 537.9 ([M+NH_4]$^+$, 100%). DCI-CH_4/HRMS Calcd for $C_{15}H_{10}ClN_2O_5{}^{187}Re$: m/z = 519.9827, found: m/z = 519.9822. UV/Vis λ_{max} (CH_3CN)/nm: 241 (ε/dm^3 mol^{-1} cm^{-1} 20000), 303 (13000), 392 (3800). Fluorescence λ_{em} (CH_3CN; λ_{exc} = 392 nm)/nm: 652.

View Article Online
DOI: 10.1039/C6DT00405A

[(bpy-COOMe)Re(CO)$_3$(CH$_3$CN)][OTf] (10). To a solution of **9** (50 mg, 96.2 µmol) in 10 mL of fresh distilled acetonitrile in the dark, under N_2, was added a solution of silver trifluoromethanesulfonate (29.5 mg, 0.115 mmol) in 1 mL of THF and the mixture was allowed to reflux overnight. The reaction mixture was filtered through a pad of Celite to remove any residual AgCl. All volatiles were removed under reduced pressure and the recrystallization was performed by layering Et_2O on a CH_2Cl_2 solution of the crude product at -18°C yielding to the desired product **10** as yellow needles (65 mg, 100%). IR ν/cm^{-1} 2039, 1924 (br), 1734. ^{1}H NMR (300 MHz; $CDCl_3$): δ 2.26 (s, 3H), 4.07 (s, 3H), 7.71 (ddd, J = 1.1, 5.5, 7.6 Hz, 1H), 8.15 (dd, J = 1.6, 5.7, 1H),), 8.30 (td, J = 1.5, 8.0 Hz, 1H), 8.66 (d, J = 8.2 Hz, 1H), 8.96 (dd, J = 0.8, 5.5 Hz, 1H), 8.99 (d, J = 0.9 Hz, 1H), 9.08 (dd, J = 0.5, 5.7 Hz, 1H). ^{19}F NMR (300 MHz; $CDCl_3$): δ -78.3. ^{13}C NMR (75 MHz; $CDCl_3$): δ 3.7 (CH_3), 53.7 (CH_3), 120.3 (q, CF_3, J = 319 Hz), 122.7 (CN), 124.5 (CH), 125.7 (CH), 127.3 (CH), 128.7 (CH), 141.3 (CH), 141.4 (Cq), 153.2 (CH), 154.0 (CH), 155.4 (Cq), 157.4 (Cq), 163.3 (C=O), 189.5 (C≡O), 193.0 (C≡O), 195.3 (C≡O). DCI-CH_4/HRMS Calcd for $C_{16}H_{10}F_3N_2O_8S^{185}Re$ [M-CH_3CN]$^+$: m/z = 631.9640, found: m/z = 631.9697. Anal. Found: C, 32.17; H, 2.04; N, 6.10. Calcd for $C_{18}H_{13}F_3N_3O_8SRe$: C, 32.05; H, 1.94; N, 6.23. UV/Vis λ_{max} (CH_3CN)/nm: 248 (ε/dm^3 mol^{-1} cm^{-1} 18000), 275 (13000), 317 (11400), 328 (11600), 359 (4600). Fluorescence λ_{em} (CH_3CN; λ_{exc} = 359 nm)/nm: 583.

[(bpy-COOMe)Re(CO)$_3$(ligand 5)][OTf] (11). To a solution of **10** (34 mg, 50.3 µmol) in THF (4 mL) in a microwave reactor was added **5** (100 mg, 124 µmol) and the mixture was heated at 105°C under microwave irradiation (155 W) for one hour. The solvent was removed *in vacuo* and the crude product was purified by chromatography over alumina (CH_2Cl_2 to CH_2Cl_2/MeOH 95:05) to provide **11** as a yellow thick oil (41 mg, 56 %). UPLC analysis: t_R = 5.07 min. IR ν/cm^{-1} 2032, 1926 (br), 1734, 1690 (br). ^{1}H NMR (300 MHz; $CDCl_3$): δ 1.43 (s, 18H), 1.44 (s, 18H), 3.51 (s, 4H), 3.52 (s, 4H), 4.04 (s, 3H), 4.10 (s, 2H), 4.13 (s, 2H), 4.59 (bs, 2H), 7.35 (d, J = 6.3 Hz, 2H), 7.58 (d, J = 7.5 Hz, 1H), 7.73 – 7.83 (m, 2H), 7.99 – 8.05 (m, 3H), 8.22 (dd, J = 1.5, 5.7 Hz, 1H), 8.27 (d, J = 7.5 Hz, 1H), 8.32 (d, J = 7.8 Hz, 1H), 8.63 (d, J = 8.1 Hz, 1H), 8.70 (d, J =1.3 Hz, 1H), 8.94 (d, J = 0.7 Hz, 1H), 9.11 (dd, J = 0.8, 5.4 Hz, 1H), 9.23 (d, J = 5.4 Hz, 1H). ^{19}F NMR (300 MHz; $CDCl_3$) δ -78.3. ^{13}C NMR (125 MHz; $CDCl_3$): δ 28.13 (CH_3), 28.14 (CH_3), 42.3 (CH_2), 53.8 (CH_3), 55.7 (CH_2), 55.8 (CH_2), 59.43 (CH_2), 59.45 (CH_2), 81.1 (Cq), 81.3 (Cq), 117.3 (CH), 119.9 (CH), 120.5 (q, CF_3, J = 319 Hz), 120.9 (CH), 122.7 (CH), 123.4 (CH), 124.8 (CH), 126.0 (CH), 126.1 (CH), 127.8

View Article Online
DOI: 10.1039/C6DT00405A

(CH), 129.2 (CH), 137.8 (CH), 141.5 (CH), 141.6 (Cq), 151.1(CH), 153.2 (Cq), 153.4 (CH), 155.2 (Cq), 157.0 (Cq), 159.78 (Cq), 159.80 (Cq), 162.9 (Cq), 165.4 (CO), 166.4 (CO), 170.4 (CO), 170.6 (CO), 190.4 (C≡O), 195.2 (C≡O), 195.3 (C≡O). ES^+/HRMS Calcd for $C_{58}H_{70}N_8O_{14}{}^{185}Re$ $[M\text{-}CF_3SO_3]^+$: m/z = 1287.4541, found: m/z = 1287.4591. UV/Vis λ_{max} (CH_3CN)/nm: 245 (ε/dm^3 mol^{-1} cm^{-1} 17500), 303 (12000), 366 (3200). Fluorescence λ_{em} (CH_3CN; λ_{exc} = 366 nm)/nm: 580.

[(Bpy-COOMe)Re(CO)$_3$(pyBPMNTA)][OTf] (12). To a stirred solution of complex **11** (40 mg, 27.8 µmol) in CH_2Cl_2 (4 mL) was added TFA (0.640 mL, 8.34 mmol) at 0°C. The mixture was then stirred 24h at room temperature. The solvent was co-evaporated several times *in vacuo* with CH_3CN to give **12** as a yellow powder (34 mg, 100 %). UPLC analysis: t_R = 1.35 min. ^{1}H NMR (400 MHz; D_2O): δ3.32-4.00 (m, 15H), 4.48 (s, 2H), 7.23 (d, J = 5.8 Hz, 2H), 7.43 (d, J = 7.8 Hz, 1H), 7.64 (s, 1H), 7.70-7.73 (m, 1H), 7.93-7.97 (m, 1H), 8.09 (d, J = 5.6 Hz, 1H), 8.17 (d, J = 6.0 Hz, 3H), 8.32-8.45 (m, 2H), 8.69 (s, 1H), 8.77 (s, 1H), 9.23 (d, J = 5.4 Hz, 1H), 9.38 (d, J = 5.6 Hz, 1H). ES^+/HRMS Calcd for $C_{42}H_{38}N_8O_{14}{}^{185}Re$ $[M\text{-}CF_3SO_3]^+$: m/z = 1063.2037, found: m/z = 1063.2039. UV/Vis λ_{max} (50 mM Tris buffer, pH 7.4)/nm: 244 (ε/dm^3 mol^{-1} cm^{-1} 16400), 304 (10900), 368 (2500). Fluorescence λ_{em} (50 mM Tris buffer, pH 7.4) λ_{exc} = 368 nm)/nm: 600.

Dinuclear Re/Gd complex 13. For preparation, see general procedure for Ln-BPMNTA complexes. Yield 36 %. The absence of free Gd(III) ion in **13** was verified using a classic test with an arsenazo indicator solution. HPLC analysis (system B); t_R = 6.9 min. UPLC analysis: t_R = 1.59 min. IR ν/cm^{-1} 2027, 1915, 1686, 1614, 1416, 1203. ES^+/HRMS Calcd for $C_{42}H_{35}N_8O_{14}ReGd$ $[M+H]^+$: m/z = 1218.1058 and 1220.1080, found: m/z = 1218.1069 and 1220.1099, respectively. UV/Vis λ_{max} (50 mM Tris buffer, pH 7.4))/nm: 247 (ε/dm^3 mol^{-1} cm^{-1} 15800), 317 (11600), 367 (2400). Fluorescence λ_{em} (50 mM Tris buffer, pH 7.4) λ_{exc} = 367 nm)/nm: 588.

Acknowledgements

The contributions of Mélanie Godeau to photophysical study of Ln-BPMNTA chelates and Sophie Laine to the structural determination of some Re complexes are gratefully acknowledged. We are grateful to Prof. R. N. Muller for his interest and support for this

View Article Online
DOI: 10.1039/C6DT00405A

current scientific work. This work was supported by the French Ministère de la Recherche (Ph.D. grant for A.B.) and the CNRS. S.L., R.N.M. and L.V.E. thank the FNRS (*Fonds National de la recherche scientifique*), and ARC Programs (AUWB-2010-10/15-UMONS-5) of the French Community of Belgium, the UIAP VII program of Belgium and the Center for Microscopy and Molecular Imaging (CMMI, supported by the European Regional Development Fund and the Walloon Region).

References

1 K. W.-Y. Chan and W.-T. Wong, *Coord. Chem. Rev.*, 2007, **251**, 2428-2451.

2 C. P. Montgomery, B. S. Murray, E. J. New, R. Pal and D. Parker, *Acc. Chem. Res.*, 2009, **42**, 925-937.

3 M. C. Heffern, L. M. Matosziuk and T. J. Meade, *Chem. Rev.*, 2014, **114**, 4496-4539.

4 E. W. Price and C. Orvig, *Chem. Soc. Rev.*, 2014, **43**, 260-290.

5 (a) Q. Zheng, H. Dai, M. E. Merritt, C. Malloy, C. Y. Pan and W.-H. Li, *J. Am. Chem. Soc.*, 2005, **127**, 16178-16188; (b) H. C. Manning, T. Goebel, R. C. Thompson, R. R. Price, H. Lee and D. J. Bornhop, *Bioconjugate Chem.*, 2004, **15**, 1488-1495.

6 (a) V. C. Pierre, M. Allen and P. Caravan, *J. Biol. Inorg. Chem.*, 2014, **19**, 127-131; (b) T. Steger-Hartmann, R. Hofmeister, R. Ernst, H. Pietsch, M. A. Sieber and J. Walter, *Invest. Radiol.*, 2010, **45**, 520-528.

7 (a) E. Debroye, S. V. Eliseeva, S. Laurent, L. Vander Elst, S. Petoud, R. N. Muller and T. N. Parac-Vogt, *Eur. J. Inorg. Chem.*, 2013, 2629-2639; (b) M. Xiao and P. R. Selvin, *J. Am. Chem. Soc.*, 2001, **123**, 7067-7073.

8 E. P. Krenning, D. J. Kwekkeboom, W. H. Bakker, W. A. P. Breeman, P. P. M. Kooij, H. Y. Oei, M. van Hagen, P. T. E. Postema, M. de Jong, J. C. Reubi, T. J. Visser, A. E. M. Reijs, L. J. Hofland, J. W. Koper and S. W. J. Lamberts, *Eur. J. Nucl. Med.*, 1993, **20**, 716-731.

9 (a) L. Koi, R. Bergmann, K. Brüchner, J. Pietzsch, H.-J. Pietzsch, M. Krause, J. Steinbach, D. Zips and M. Baumann, *Radiother. Oncol.*, 2014, **110**, 362-369; (b) R. Haubner, D. R. Vera, S. Farshchi-Heydari, A. Helbok, C. Rangger, D. Putzer and I. J. Virgolini, *Eur. J. Nucl. Med. Mol. Imaging*, 2013, **40**, 1245-1255.

10 (a) E. W. Price, B. M. Zeglis, J. F. Cawthray, C. F. Ramogida, N. Ramos, J. S. Lewis, M. J. Adam and C. Orvig, *J. Am. Chem. Soc.*, 2013, **135**, 12707-12721; (b) C. Platas-Iglesias, M. Mato-Iglesias, K. Djanashvili, R. N. Muller, L. Vander Elst, J. A. Peters, A. de Blas and T. Rodriguez-Blas, *Chem. Eur. J.*, 2004, **10**, 3579-3590; (c) F. K. Kalman, A. Végh, M.

Regueiro-Figueroa, E. Toth, C. Platas-Iglesias and G. Tircso, *Inorg. Chem.*, 2015, **54**, 2345-2356.

11 S. Laurent, L. Vander Elst, C. Galaup, N. Leygue, S. Boutry, C. Picard and R. N. Muller, *Contrast Media Mol. Imaging*, 2014, **9**, 300-312.

12 F. Havas, M. Danel, C. Galaup, P. Tisnès and C. Picard, *Tetrahedron Lett.*, 2007, **48**, 999-1002.

13 S. Brillouet, S. Dorbes, F. Courbon, C. Picard, J. P. Delord, E. Benoist, M. Poirot, B. Mestre-Voegtlé and S. Silvente-Poirot, *Bioorg. Med. Chem.*, 2010, **18**, 5400–5412.

14 A. Thibon and V. C. Pierre, *Anal. Bioanal. Chem.*, 2009, **394**, 107–120.

15 D. Guillaumont, H. Bazin, J.-M. Benech, M. Boyer and G. Mathis, *ChemPhysChem*, 2007, **8**, 480-488.

16 (a) T. Koullourou, L. S. Natrajan, H. Bhavsar, S. J. A. Pope, J. Feng, J. Narvainen, R. Shaw, E. Scales, R. Kauppinen, A. M. Kenwright and S. Faulkner, *J. Am. Chem. Soc.*, 2008, **130**, 2178-2179; (b) M. Tropiano, C. J. Record, E. Morris, H. S. Rai, C. Allain and S. Faulkner, *Organometallics*, 2012, **31**, 5673-5676.

17 A. Boulay, S. Laine, N. Leygue, E. Benoist, S. Laurent, L. Vander Elst, R. N. Muller, B. Mestre-Voegtlé and C. Picard, *Tetrahedron Lett.*, 2013, **54**, 5395-5398.

18 F. Havas, N. Leygue, M. Danel, B. Mestre, C. Galaup and C. Picard, *Tetrahedron*, 2009, **65**, 7673-7686.

19 J. S. Josan, C. R. De Silva, B. Yoo, R. M. Lynch, M. D. Pagel, J. Vagner and V. J. Hruby, *Methods Mol. Biol.*, 2011, **716**, 89-126.

20 (a) A. Beeby, I. M. Clarkson, R. S. Dickins, S. Faulkner, D. Parker, L. Royle, A. S. de Sousa, J. A. G. Williams and M. Woods, *J. Chem. Soc., Perkin Trans. 2*, 1999, 493-503; (b) R. M. Supkowski and W. D. W. Horrocks Jr., *Inorg. Chim. Acta*, 2002, **340**, 44-48.

21 V. L. Ermolaev and E. B. Sveshnikova, *Russ. Chem. Rev.*, 1994, **63**, 905-922.

22 (a) M. Latva, H. Takalo, V.-M. Mukkala, C. Matachescu, J.-C. Rodriguez-Ubis and J. Kankare, *J. Lumin.*, 1997, **75**, 149-169; (b) N. Weibel, L. J. Charbonnière, M. Guardigli, A. Roda and R. Ziessel, *J. Am. Chem. Soc.*, 2004, **126**, 4888-4896. (c) I. Nasso, C. Galaup, F. Havas, P. Tisnès, C. Picard, S. Laurent, L. Vander Elst and R. N. Muller, *Inorg. Chem.*, 2005, **44**, 8293-8305.

23 N. Sabbatini, M. Guardigli and J.-M. Lehn, *Coord. Chem. Rev.*, 1993, **123**, 201-228.

24 F. J. Steemers, W. Verboom, D. N. Reinhoudt, E. B. van der Tol and J. W. Verhoeven, *J. Am. Chem. Soc.*, 1995, **117**, 9408-9414.

25 J.-C. G. Bünzli, *Coord. Chem. Rev.*, 2015, **293-294**, 19-47.

26 (a) T. Ito, M. Inoue, K. Akamatsu, E. Kusaka, K. Tanabe and S.-I. Nishimoto, *Bioorg. Med. Chem. Lett.*, 2011, **21**, 3515-3518; (b) J.-M. Couchet, J. Azéma, C. Galaup and C. Picard, *J. Lumin.*, 2011, **131**, 2735–2745; (c) G. Bechara, N. Leygue, C. Galaup, B. Mestre-Voegtlé and C. Picard, *Tetrahedron*, 2010, **66**, 8594-8604; (d) L. Charbonnière, R. Ziessel, M. Guardigli, A. Roda, N. Sabbatini and M. Cesario, *J. Am. Chem. Soc.*, 2001, **123**, 2436-2437; (e) C. Galaup, M.-C. Carrié, P. Tisnès and C. Picard, *Eur. J. Org. Chem.*, 2001, 2165-2175.

27 J.-C. G. Bünzli, *Chem. Rev.*, 2010, **110**, 2729-2755.

28 (a) A. Beeby, L. M. Bushby, D. Maffeo and J. A. G. Williams, *J. Chem. Soc., Dalton Trans.*, 2002, 48-54.; (b) M. H. V. Werts, R. T. F. Jukes and J. W. Verhoeven, *Phys. Chem. Chem. Phys.*, 2002, **4**, 1542-1548.

29 (a) G. Dehaen, S. V. Eliseeva, P. Verwilst, S. Laurent, L. Vander Elst, R. N. Muller, W. De Borggraeve, K. Binnemans and T. N. Parac-Vogt, *Inorg. Chem.*, 2012, **51**, 8775-8783; (b) A. D'Aléo, M. Allali, A. Picot, P. L. Baldeck , L. Toupet , C. Andraud and O. Maury, *C. R. Chimie*, 2010, **13**, 681–690.

30 G. Mathis and H. Bazin in *Lanthanide Luminescence (Photophysical, Analytical and Biological Aspect)*, ed. P. Hanninen and H. Harma, Springer, 2011, ch. 2, pp 47- 88.

31 A. E. Martell and R. M. Smith in *Critical stability constants*, Plenum Press, New York and London, 1974, vol.1, p 205.

32 M. H. V. Werts, J. W. Verhoeven and J. W. Hofstraat, *J. Chem. Soc., Perkin Trans. 2*, 2000, 433-439.

33 S. Laurent, L. Vander Elst and R. N. Muller, *Contrast Media Mol. Imaging*, 2006, **1**, 128-137.

34 P. Caravan, *Chem. Soc. Rev.*, 2006, **35**, 512-523.

35 (a) L. Vander Elst, F. Maton, S. Laurent, F. Seghi, F. Chapelle and R. N. Muller, *Magn. Reson. Med.*, 1997, **38**, 604-614; (b) R. N. Muller, B. Radüchel, S. Laurent, J. Platzek, C. Piérart, P. Mareski and L. Vander Elst, *Eur. J. Inorg. Chem.*, 1999, 1949-1955.

36 M. Woods, M. Botta, S. Avedano, J. Wang and A. D. Sherry, *Dalton Trans.*, 2005, 3829-3837.

37 P. Hermann, J. Kotek, V. Kubicek and I. Lukes, *Dalton Trans.*, 2008, 3027-3047.

38 S. Aime, M. Botta, M. Fasano and E. Terreno, *Chem. Soc. Rev.*, 1998, **27**, 19-29.

39 K. Micskei, L. Helm, E. Brucher and A. E. Merbach, *Inorg. Chem.*, 1993, **32**, 3844-3850.

40 S. Laurent, C. Henoumont, L. Vander Elst and R. N. Muller, *Eur. J. Inorg. Chem.*, 2012, 1889-1915.

41 V. Henrotte, L. Vander Elst, S. Laurent and R. N. Muller, *J. Biol. Inorg. Chem.*, 2007, **12**, 929–937.

42 S. Silverio, S. Torres, A. F. Martins, J. A. Martins, J. P. Andre, L. Helm, M. I. M. Prata, A. C. Santos and C. F. G. C. Geraldes, *Dalton Trans.*, 2009, 4656-4670.

43 See for examples: (a) T. S. Pitchumony, L. Banevicius, N. Janzen, J. Zubieta and J. F. Valliant, *Inorg. Chem.*, 2013, **52**, 13521-13528; (b) K. Yin Zhang, K. K.-S. Tso, M.-W. Louie, H.-W. Liu and K. K.-W. Lo, *Organometallics*, 2013, **32**, 5098-5102; (c) V. Fernandez-Moreira, M. L. Ortego, C. F. Williams, M. P. Coogan, M. D. Villacampa and M. C. Gimeno, *Organometallics*, 2012, **31**, 5950-5957; (d) V. Fernandez-Moreira, F. L. Thorp-Greenwood, A. J. Amoroso, J. Cable, J. B. Court, V. Gray, A. J. Hayes, R. L. Jenkins, B. M. Kariuki, D. Lloyd, C. O. Millet, C. F. Williams and M. P. Coogan, *Org. Biomol. Chem.*, 2010, **8**, 3888-3901; (e) D. Lloyd, M. P. Coogan and S. J. A Pope, *Reviews in Fluorescence* 2010, **7**, 15-44.

44 A. Boulay, M. Artigau, Y. Coulais, C. Picard, B. Mestre-Voegtlé and E. Benoist, *Dalton Trans.*, 2011, **40**, 6206-6209.

45 (a) M.-W. Louie, M. H.-C. Lam and K. K.-W. Lo, *Eur. J. Inorg. Chem.*, 2009, 4265-4273; (b) A. J. Amoroso, M. P. Coogan, J. E. Dunne, V. Fernandez-Moreira, J. B. Hess, A. J. Hayes, D. Lloyd, C. Millet, S. J. A. Pope and C. Williams, *Chem. Commun.*, 2007, 3066-3068; (c) M. Gottschaldt, D. Koth, D. Müller, I. Klette, S. Rau, H. Görls, B. Schäfer, R. P. Baum and S. Yano, *Chem. Eur. J.*, 2007, **13**, 10273-10280.

46 (a) M. D. Doherty, D. C. Grills and E. Fujita, *Inorg. Chem.*, 2009, **48**, 1796-1798; (b) R. F. Semeniuc, T. J. Reamer, J. P. Blitz, K. A. Wheeler and M. D. Smith, *Inorg. Chem.*, 2010, **49**, 2624-2629.

47 S. Clède, F. Lambert, C. Sandt, Z. Gueroui, M. Réfrégiers, M.-A. Plamont, P. Dumas, A. Vessières and C. Policar, *Chem. Commun.*, 2012, **48**, 7729–7731.

48. Y. Haas and G. Stein, *J. Phys. Chem.*, 1971, **75**, 3668-3677.

49. H. Ishida, S. Tobita, Y. Hasegawa, R. Katoh and K. Nozaki, *Coord. Chem. Rev.*, 2010, **254**, 2449-2458.

50. S. R. Meech and D. Phillips, *J. Photochem.*, 1983, **23**, 193-217.

51. R. N. Muller, D. Declercq, P. Vallet, F. Giberto, B. Daminet, H. W. Fisher, F. Maton and Y. Van Haverbeke, Proceedings of the ESMRMB, 7th Annual Congress, Strasbourg, France, 1990, p 394.

52. P. Vallet, Ph. D. Thesis, University of Mons, Belgium, 1992.

53. D. Pérez, G. Burés, E. Guitian and L. Castedo, *J. Org. Chem.*, 1996, **61**, 1650-1654.

View Article Online
DOI: 10.1039/C6DT00405A

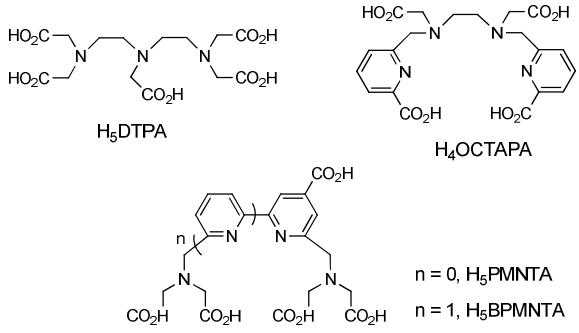

Fig.1 Chemical structures of the ligands discussed in this work.

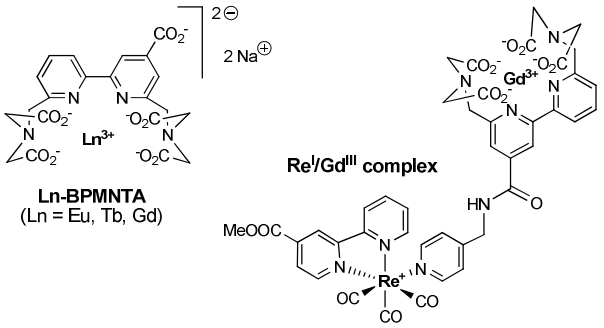

Fig. 2 Schematic representation of Ln-BPMNTA complexes and dinuclear Re^{I}/Gd^{III} complex.

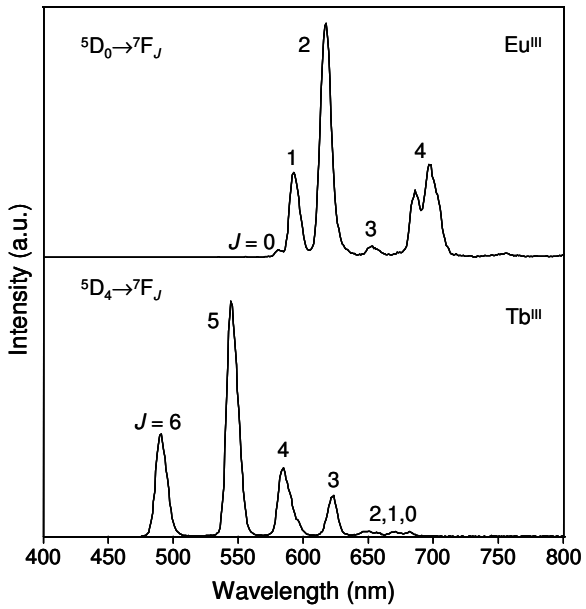

Fig.3 Corrected and normalized emission spectra of Eu-BPMNTA and Tb-BPMNTA complexes in Tris buffer (pH 7.4) under excitation at 316 nm at 298 K

View Article Online
DOI: 10.1039/C6DT00405A

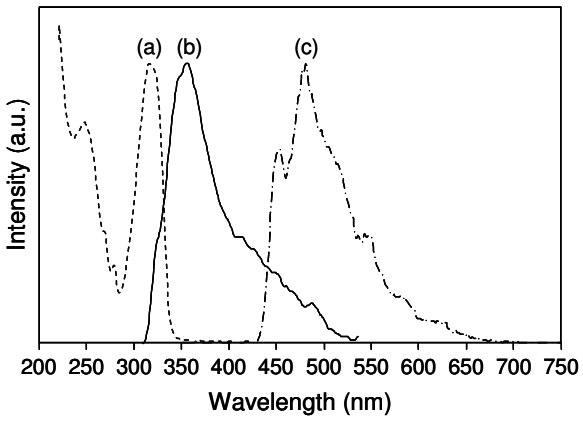

Fig.4 Normalized (a) absorption (- - -), (b) fluorescence (——) and (c) phosphorescence (-·-·-) spectra of Gd-BPMNTA complex. The absorption and fluorescence spectra were measured at 298 K in Tris buffer (pH 7.4) and the phosphorescence spectrum at 77 K in Tris buffer-glycerol (4:1 v/v) glassy matrix.

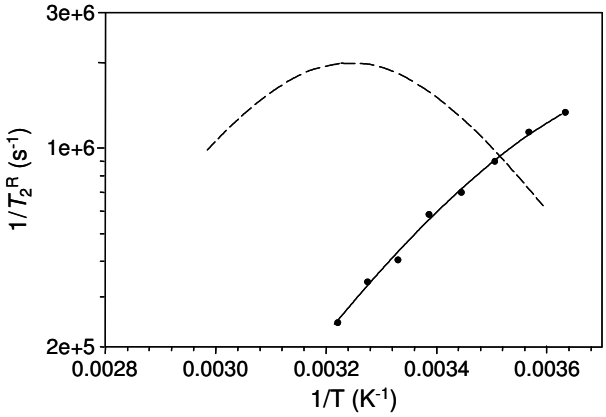

Fig.5 ^{17}O reduced transverse relaxation rate ($1/T_2^R$) as a function of the reciprocal of the temperature for aqueous solution of Gd-BPMNTA (solid circles) at 500 MHz. The solid line corresponds to the theoretical fitting of the data points. The dashed line corresponds to the fitting of Gd-DTPA data.

View Article Online
DOI: 10.1039/C6DT00405A

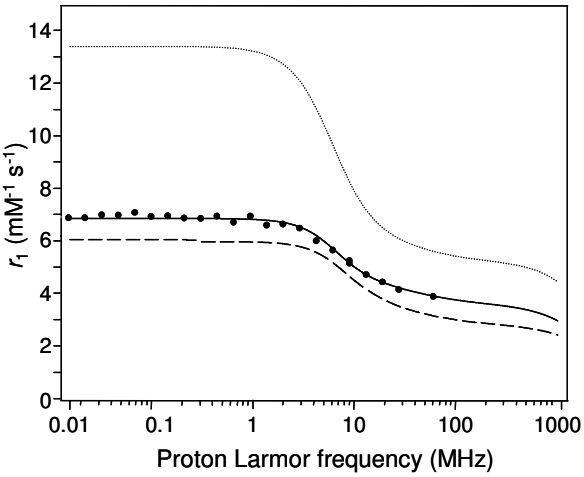

Fig.6 ^{1}H NMRD relaxivity profile of Gd-BPMNTA (solid circles) in water at 310 K. The solid line through the data corresponds to the theoretical fitting. The dotted and dashed lines correspond to the fitting of Gd-PMNTA and Gd-DTPA data, respectively.

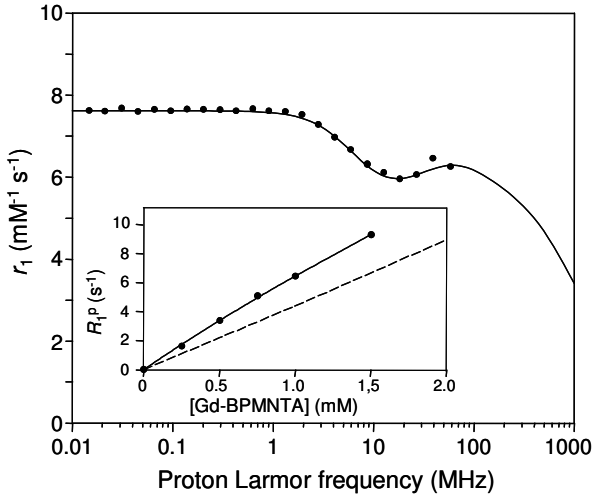

Fig.7 ^{1}H NMRD profile of Gd-BPMNTA complex at a concentration of 1 mM in the presence of 4% HSA at 310K. Inset: Proton paramagnetic relaxation rate of aqueous 4% HSA solution containing increasing amounts of Gd-BPMNTA at 20 MHz and 310 K; the continuous line corresponds to the fitting of the data and the dashed line represents R_1^p in a water solution free of HSA.

View Article Online
DOI: 10.1039/C6DT00405A

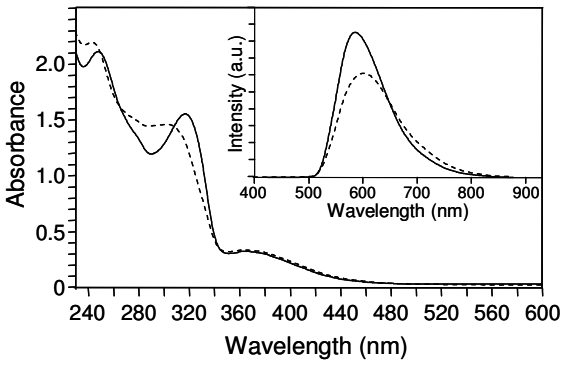

Fig.8 Absorption spectra of complexes **12** (- - -) and **13** (——) in aerated Tris buffer (pH 7.4). Inset: emission spectra of complexes **12** (- - -) and **13** (——) at 298 K in aerated Tris buffer (pH 7.4).

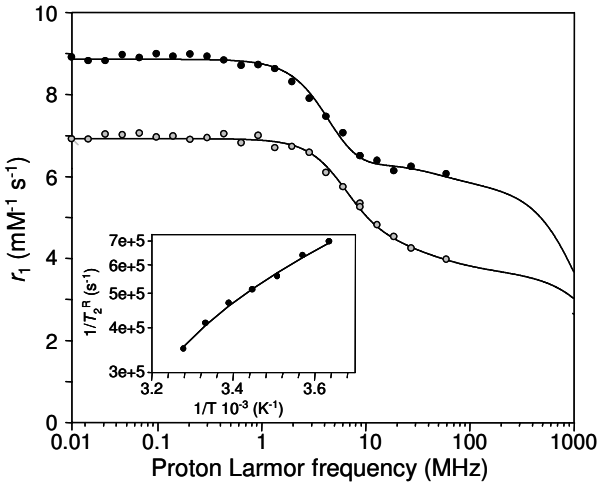

Fig. 9 ^{1}H NMRD relaxivity profiles of dinuclear Re^{I}/Gd^{III} complex **13** (black circles) and Gd-BPMNTA (grey circles) in water at 310 K. The continuous lines correspond to the theoretical fitting of the data points. Inset: ^{17}O reduced transverse relaxation rate ($1/T_2^R$) as a function of the reciprocal of the temperature for aqueous solution of complex **13** (solid circles) at 500 MHz; the line corresponds to the theoretical fitting.

View Article Online
DOI: 10.1039/C6DT00405A

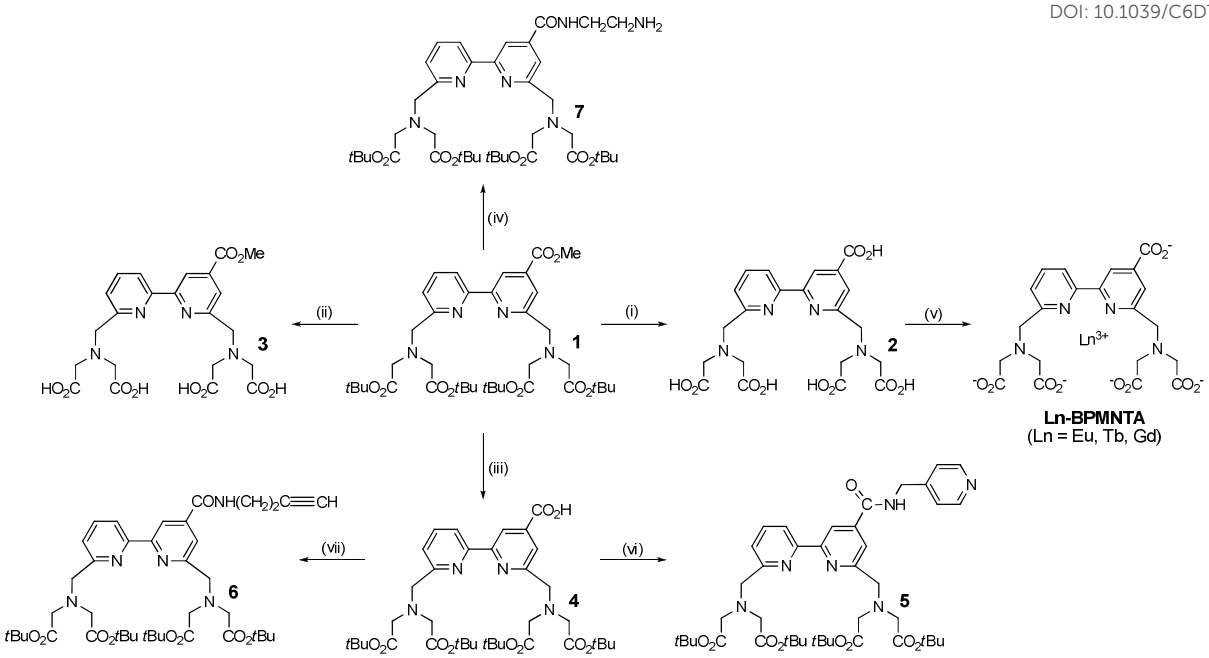

Scheme 1 *reagents and conditions*: (i) HCl 6M, 90°C, 4 d, 100%; (ii) CF_3COOH, CH_2Cl_2, rt, 18 h, 87%; (iii) LiOH, THF/H_2O, rt, 2 h, 89%; (iv) $H_2NCH_2CH_2NH_2$, rt, 24 h, 100%; (v) $LnCl_3$, H_2O, pH 5-6, rt, overnight, 100%; (vi) 4-(aminomethyl)pyridine, PyBOP, DIPEA, CH_2Cl_2, rt, 48 h, 79%; (vii) but-3-yn-1-amine hydrochloride, PyBOP, DIPEA, CH_2Cl_2, rt, 24 h, 72%.

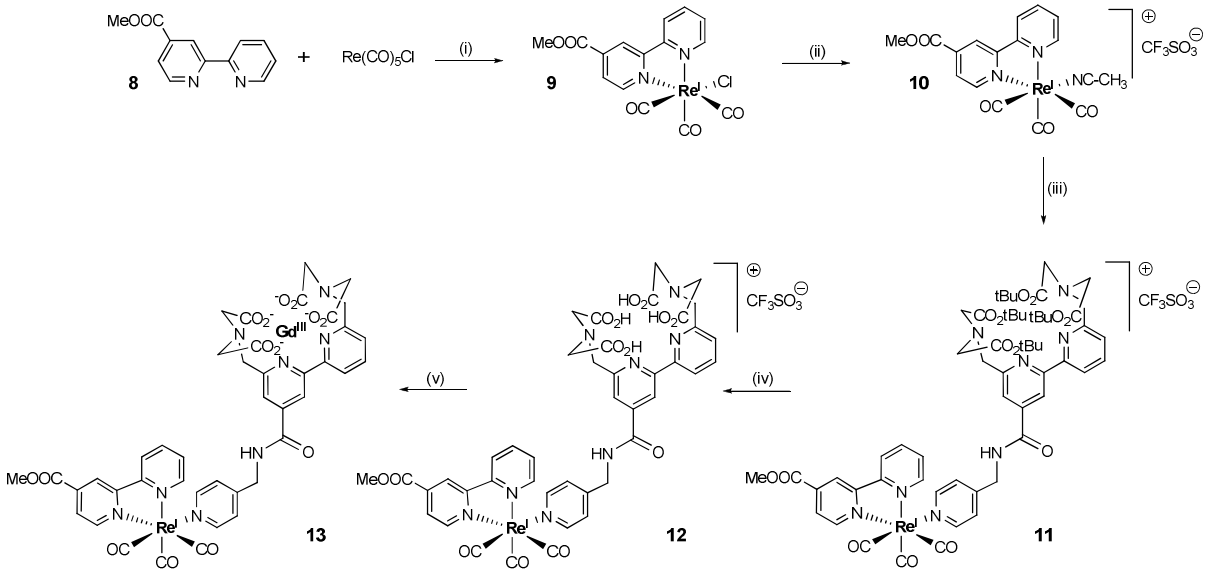

Scheme 2 *reagents and conditions*: (i) $Re(CO)_5Cl$, MeOH, 65°C, overnight, 91%; (ii) AgOTf, THF/CH_3CN, reflux, overnight, 100%; (iii) compound **5**, THF, MW (155 W), 1 h, 56%; (iv) CF_3COOH, CH_2Cl_2, rt, 24 h, 100%; (v) $GdCl_3$, H_2O, pH 5-6, rt, overnight, 36%.

View Article Online
DOI: 10.1039/C6DT00405A

Table 1 Absorption and metal luminescence data of Eu-BPMNTA and Tb-BPMNTA in aerated Tris buffer (50 mM, pH 7.4) solutions

Compd	$\pi\rightarrow\pi^*$ λ_{max}/nm (log ε)	λ_{em}/nm	τ_{H_2O}/ms [a] 298 K (77 K)	τ_{D_2O}/ms [a] 298 K (77 K)	k_{nr}(OH) [b] (s^{-1})	k_{nr}(T) [c] (s^{-1})	q [d] 298 K	Φ_{ov} (%)[e]
Eu-BPMNTA	246 (4.02), 316 (4.09)	617	0.60 (1.08)	2.22 (2.29)	1200	10	1.0	12.9
Tb-BPMNTA	246 (3.98), 316 (4.08)	544	0.51 (1.94)	0.58 (2.65)	240	1350	0.9	10

[a] Determined by excitation into the lowest-energy ligand-centred absorption band and recording the intensity of the $^5D_0\rightarrow{}^7F_2$ (617 nm), $^5D_4\rightarrow{}^7F_5$ (544 nm) for Eu^{III}, Tb^{III}, respectively. [b] $k_{nr}(OH) = (\tau_{H_2O})^{-1} - (\tau_{D_2O})^{-1}$. [c] $k_{nr}(T) = (\tau_{D_2O,\,298\,K})^{-1} - (\tau_{D_2O,\,77\,K})^{-1}$. [d] Number of coordinated H_2O molecules: $q_{H_2O}(Eu) = 1.11[(\tau_{H_2O})^{-1} - (\tau_{D_2O})^{-1} - 0.31]$[20b], $q_{H_2O}(Tb) = 5[(\tau_{H_2O})^{-1} - (\tau_{D_2O})^{-1} - 0.06]$[20a], with lifetimes in ms. [e] Overall quantum yields were determined under ligand excitation.

Table 2 Parameters obtained from the theoretical fitting of the O-17 data for Gd-BPMNTA complex in water at 11.75 T

parameter	value
τ_M^{310K} [ns]	3.9 ± 0.2
$\Delta H^{\neq}$ [kJ mol^{-1}]	52.0 ± 0.8
$\Delta S^{\neq}$ [J mol^{-1} K^{-1}]	83.7 ± 0.3
$A/\hbar$ [10^6 rad s^{-1}]	-3.9 ± 0.03
B [10^{20} s^{-2}]	3.25 ± 0.1
τ_v^{298K} [ps]	2.25 ± 0.1
E_v [kJ mol^{-1}]	14.2 ± 1.7

Table 3 Relaxivity values at 20 and 60 MHz (T = 310 K) and parameters obtained from the theoretical fitting of the proton NMRD data in water at 310 K for Gd-BPMNTA complex and related complexes

parameter	Gd-BPMNTA	Gd-PMNTA[a]	Gd-OCTAPA[b]	Gd-DTPA[c]
τ_M^{310K} [ns]	3.9 ± 0.2	38.5 ± 10.5	200	143 ± 25
τ_R^{310K} [ps]	76 ± 2.3	64 ± 2	55 ± 10	54 ± 1.4
τ_{SO}^{310K} [ps]	78 ± 2.0	194 ± 14	-	87 ± 3
τ_V^{310K} [ps]	21.8 ± 1.8	21.7 ± 4.1	-	25 ± 3
r_1 (mM^{-1} s^{-1}) at 20 MHz	4.4	6.4	5.0	3.8
r_1 (mM^{-1} s^{-1}) at 60 MHz	4.0	5.7	-	3.4

[a] from ref 11. [b] values at 298 K from ref 10b. [c] from ref 33.

View Article Online
DOI: 10.1039/C6DT00405A

Table 4 Photophysical data of Re^{I} complexes **9**-**13**

Compd	Medium	λ_{abs}/nm (log ε)	λ_{em}/nm	Φ (%)
9	CH_3CN	241 (4.3), 303 (4.11) 392 (3.58)	652	0.15
10	CH_3CN	248 (4.26), 275 (4.11) 317 (4.05), 328 (4.06) 359 (3.66)	583	2.3
11	CH_3CN	245 (4.24), 303 (4.08) 366 (3.51)	580	2.0
12	Tris buffer pH 7.4	244(4.22), 304 (4.04) 368 (3.40)	600	1.2
13	Tris buffer pH 7.4	247 (4.20), 317 (4.07) 367 (3.38)	588	1.4

View Article Online
DOI: 10.1039/C6DT00405A

Optical and relaxometric properties of monometallic (Eu^{III}, Tb^{III}, Gd^{III}) and heterobimetallic (Re^{I}/Gd^{III}) systems based on a functionalized bipyridine-containing acyclic ligand

Nadine Leygue, Alexandre Boulay, Chantal Galaup, Eric Benoist, Sophie Laurent, Luce Vander Elst, Béatrice Mestre-Voegtlé and Claude Picard

The photophysical and relaxometric properties in aqueous solutions of Ln-BPMNTA complexes and a derived Re^{I}/Gd^{III} dinuclear complex are reported.